Geological Society of America
Special Paper 371
2003

Geologic signature of early Tertiary ridge subduction in Alaska

Dwight Bradley*
U.S. Geological Survey, 4200 University Drive, Anchorage, Alaska 99508, USA

Tim Kusky
Department of Earth and Atmospheric Sciences, St. Louis University, St. Louis, Missouri 63103, USA

Peter Haeussler
U.S. Geological Survey, 4200 University Drive, Anchorage, Alaska 99508, USA

Rich Goldfarb
U.S. Geological Survey, Box 25046, MS 973, Denver Federal Center, Denver, Colorado 90225, USA

Marti Miller
Julie Dumoulin
Steven W. Nelson
Sue Karl
U.S. Geological Survey, 4200 University Drive, Anchorage, Alaska 99508, USA

ABSTRACT

A mid-Paleocene to early Eocene encounter between an oceanic spreading center and a subduction zone produced a wide range of geologic features in Alaska. The most striking effects are seen in the accretionary prism (Chugach–Prince William terrane), where 61 to 50 Ma near-trench granitic to gabbroic plutons were intruded into accreted trench sediments that had been deposited only a few million years earlier. This short time interval also saw the genesis of ophiolites, some of which contain syngenetic massive sulfide deposits; the rapid burial of these ophiolites beneath trench turbidites, followed immediately by obduction; anomalous high-*T*, low-*P*, near-trench metamorphism; intense ductile deformation; motion on transverse strike-slip and normal faults; gold mineralization; and uplift of the accretionary prism above sea level. The magamatic arc experienced a brief flare-up followed by quiescence. In the Alaskan interior, 100 to 600 km landward of the paleotrench, several Paleocene to Eocene sedimentary basins underwent episodes of extensional subsidence, accompanied by bimodal volcanism. Even as far as 1000 km inboard of the paleotrench, the ancestral Brooks Range and its foreland basin experienced a pulse of uplift that followed about 40 million years of quiescence.

All of these events—but most especially those in the accretionary prism—can be attributed with varying degrees of confidence to the subduction of an oceanic spreading center. In this model, the ophiolites and allied ore deposits were produced at the soon-to-be subducted ridge. Near-trench magmatism, metamorphism, deformation, and gold mineralization took place in the accretionary prism above a slab window, where hot asthenosphere welled up into the gap between the two subducted, but still diverging, plates. Deformation took place as the critically tapered accretionary prism

*dbradly@usgs.gov

Bradley, D., Kusky, T., Haeussler, P., Goldfarb, R., Miller, M., Dumoulin, J., Nelson, S.W., and Karl, S., 2003, Geologic signature of early Tertiary ridge subduction in Alaska *in* Sisson, V.B., Roeske, S.M., and Pavlis, T.L., eds., Geology of a transpressional orogen developed during ridge-trench interaction along the North Pacific margin: Boulder, Colorado, Geological Society of America Special Paper 371, p. X–XX.

adjusted its shape to changes in the bathymetry of the incoming plate, changes in the convergence direction before and after ridge subduction, and changes in the strength of the prism as it was heated and then cooled. In this model, events in the Alaskan interior would have taken place above more distal, deeper parts of the slab window. Extensional (or transtensional) basin subsidence was driven by the two subducting plates that each exerted different tractions on the upper plate. The magmatic lull along the arc presumably marks a time when hydrated lithosphere was not being subducted beneath the arc axis. The absence of a subducting slab also may explain uplift of the Brooks Range and North Slope: Geodynamic models predict that long-wavelength uplift of this magnitude will take place far inboard from Andean-type margins when a subducting slab is absent. Precise correlations between events in the accretionary prism and the Alaskan interior are hampered, however, by palinspastic problems. During and since the early Tertiary, margin-parallel strike-slip faulting has offset the near-trench plutonic belt—i.e., the very basis for locating the triple junction and slab window—from its backstop, by an amount that remains controversial.

Near-trench magmatism began at 61 Ma at Sanak Island in the west but not until 51 Ma at Baranof Island, 2200 km to the east. A west-to-east age progression suggests migration of a trench-ridge-trench triple junction, which we term the Sanak-Baranof triple junction. Most workers have held that the subducted ridge separated the Kula and Farallon plates. As a possible alternative, we suggest that the ridge may have separated the Kula plate from another oceanic plate to the east, which we have termed the Resurrection plate.

Keywords: massive sulfide deposits, gold mineralization, brittle faulting, accretionary prism, ridge subduction, Chugach–Prince William terrane, Sanak Island, triple junction.

INTRODUCTION

Southern Alaska has a long history as a convergent margin, where various plates of the Pacific Ocean have been subducted. During much of the time since the Jurassic, it is possible to recognize the same standard elements of a subduction zone that are seen today: backarc, magmatic arc, forearc basin, and accretionary prism. Each of these elements underwent major changes in the early Tertiary. The most striking changes were in the accretionary prism, where near-trench granodiorite plutons—some of batholithic proportions—were intruded into accreted trench deposits that had been deposited only a few million years earlier (Moore et al., 1983) (Figs. 1 and 2). At this same time, the accretionary prism was metamorphosed at high-*T*, low-*P* conditions (Sisson et al., 1989), ductilely deformed over large regions (Pavlis and Sisson, 1995), cut by strike-slip and normal faults (Kusky et al., 1997a), and mineralized by gold-bearing hydrothermal systems (Haeussler et al., 1995). Meanwhile, very young ophiolites were accreted onto the leading edge of the subduction complex (Kusky and Young, 1999). It was an unusual time in the history of the convergent margin, presumably due to special circumstances.

One important clue to the cause of early Tertiary events in Alaska can be found offshore, in the magnetic anomalies of the northern Pacific plate. A ~70-degree bend in the anomaly pattern, known as the Great Magnetic Bight, implies that three oceanic plates existed here in the early Tertiary, separated by three spreading ridges (Atwater, 1989). One ridge, between the Kula and Farallon plates, headed in the general direction of North America—but exactly where it intersected the margin cannot be deciphered from marine magnetic anomalies, because all of the evidence has been subducted (Page and Engebretson, 1984; Atwater, 1989). The track of a migrating trench-ridge-trench triple junction is suggested, however, by the near-trench plutons in Alaska. As will be shown, ridge subduction provides the most reasonable explanation for these plutons, which define the Sanak-Baranof plutonic belt of Hudson et al. (1979). If the Great Magnetic Bight is a smoking gun, the near-trench plutons would then be the bullet holes. In fact, ridge subduction provides such an elegant rationale for the age, location, and geochemistry of these plutons that since being first proposed a quarter-century ago (Marshak and Karig, 1977), it has become the leading hypothesis (e.g., Helwig and Emmet, 1981; Hill et al., 1981; Moore et al., 1983; Barker et al., 1992; Sisson and Pavlis, 1993; Bradley et al., 1993; Pavlis and Sisson, 1995; Haeussler et al., 1995; Poole, 1996; Harris et al., 1996).

The case for early Tertiary ridge subduction in Alaska has not been universally embraced. For example, Engebretson's (1985) widely cited plate reconstructions showed the Kula-Farallon ridge being subducted at the latitude of Washington, and no ridge-trench interactions in Alaska. In Plafker and Berg's 1994 Decade of North American Geology synthesis of Alaskan tectonic evolution, they likewise showed no ridge intersecting the Alaskan margin during the time in question. Various alternative explanations for the near-trench plutons—published and unpublished—have been put forth: They were emplaced along an arc that had jumped to an extreme trenchward position (Kienle and Turner, 1976); they record anatectic melting of a thick pile of recently subducted flysch (Hudson et al., 1979); the trench

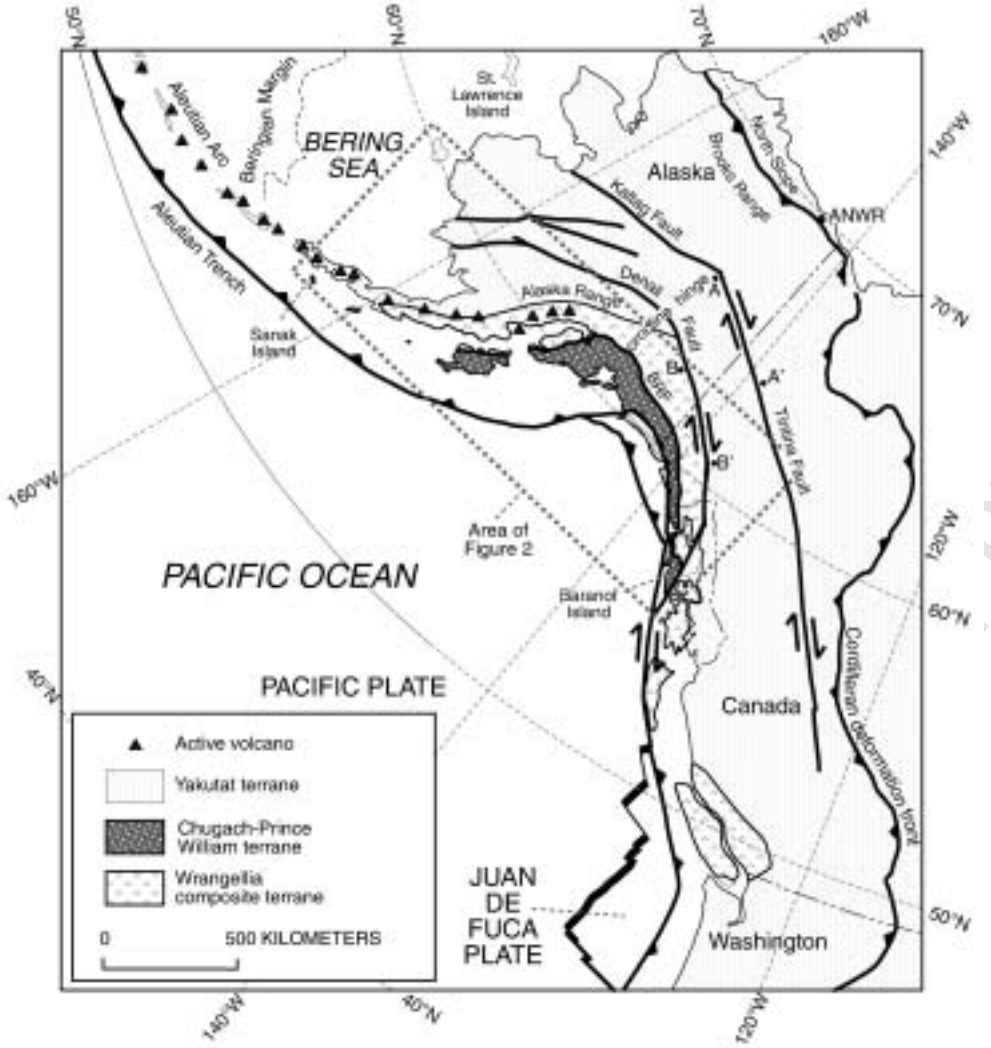

Figure 1. Map of Alaska and surrounding areas showing geologic features mentioned in text. A and A' mark offset across Tintina fault system (after Dover, 1994); B and B' mark offset across Denali fault (Lowey, 1998). Wrangellia composite terrane includes Wrangellia, Alexander, and Peninsular terranes.

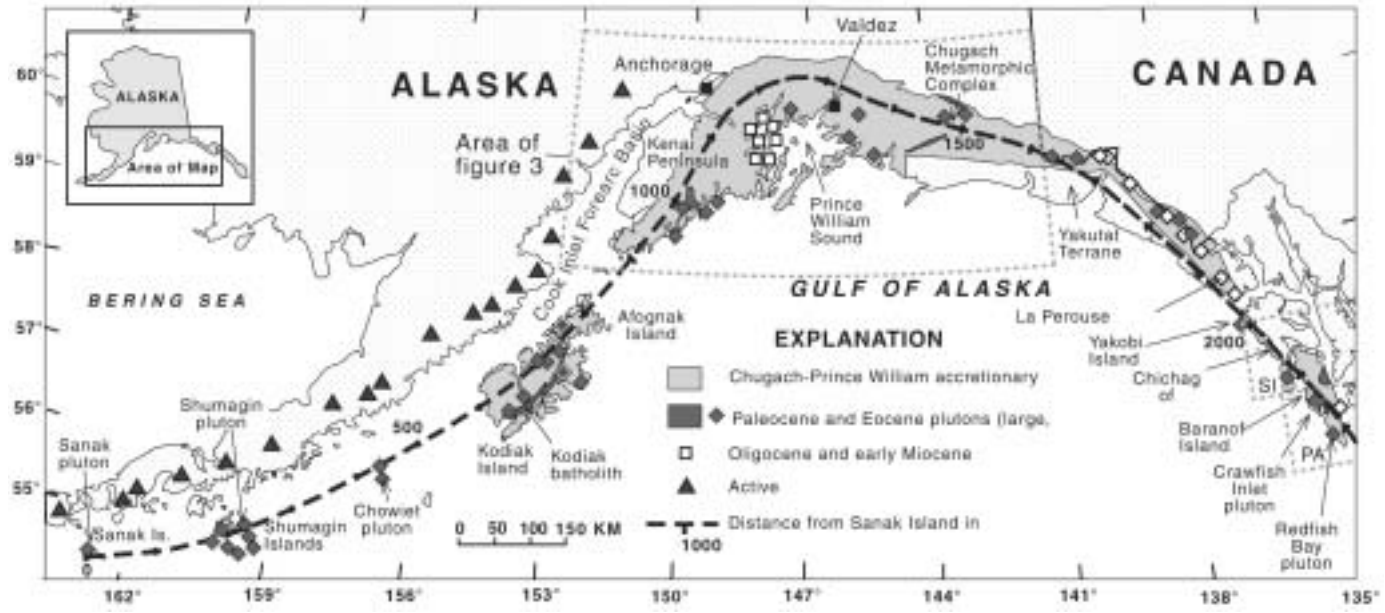

Figure 2. Map of the Chugach–Prince William terrane showing locations of Sanak-Baranof near-trench intrusive rocks. Abbreviations: SI—Sitka quadrangle; PA—Port Alexander quadrangle.

overrode a hotspot; very young, hot, oceanic lithosphere was subducted; a "leaky transform" entered the trench (Tysdal et al., 1977); near-trench magmatism was the product of flexural extension of a single downgoing plate (Tysdal et al., 1977); and a subducted slab broke off, exposing the overriding plate to a slab window. As will be discussed at greater length below, the evidence now in hand is best explained by the ridge subduction hypothesis. Accordingly, as this volume itself makes clear, the emphasis of current research has shifted from testing alternative tectonic scenarios, to refining the ridge subduction scenario and studying processes of ridge subduction. By analogy, studies of the Franciscan Complex have long since advanced beyond the question of whether or not it is the product of subduction, to questions about subduction zones. Still, it behooves us to not forget alternative explanations that are no longer in the forefront. This philosophy guides the first part of the present paper, a non-interpretive discussion of Alaska's early Tertiary geologic record.

Our descriptive overview of the geology is based on our own experience gained through field work during the past two decades, as well as on published findings. Most of our work was done in connection with 1:250,000-scale reconnaissance bedrock mapping and resource assessment by the U.S. Geological Survey in the Seldovia, Seward, Cordova, Valdez, Sitka, Port Alexander, Talkeetna, and Talkeetna Mountains quadrangles (Figs. 2 and 3). We emphasize geology of the accretionary prism, rocks most pertinent to the subduction history. Specific aspects of the early Tertiary geology of the accretionary prism have been discussed in several dozen publications—but a comprehensive synthesis has been lacking. The early Tertiary record of interior Alaska is covered here in less detail, because new research has just been started that will quickly eclipse our present knowledge. In the Alaskan interior, various episodes of early Tertiary basin subsidence, uplift, magmatism, and mineralization attest to significant tectonic activity that presumably was related to events along the continental margin—but reliable correlations must await tighter dating and new information on the amount of margin-parallel strike slip.

The second part of the paper is interpretive. Here we present the case that ridge subduction provides a unifying rationale for the broad range of evidence, and we consider the various competing, but to us less satisfactory, hypotheses. We conclude with some general observations about ridge subduction, and a discussion of some outstanding problems in Alaska.

GEOLOGIC SETTING

Alaska consists of a collage of terranes that were accreted to the western margin of North America as a result of complex plate interactions through most of the Phanerozoic. Comprehensive reviews and bibliographies of the regional geology are given by Plafker et al. (1994) and Nokleberg et al. (1994). Those terranes of particular significance to the present study are introduced here along a south-to-north transect along the hinge of the southern Alaska orocline (Fig. 1). Alaska's Pacific margin is underlain by a Mesozoic and Cenozoic accretionary prism, referred to as the Chugach–Prince William terrane (or composite terrane), which is discussed in more detail below. It was built in piecemeal fashion by subduction-accretion and lies seaward of the Wrangellia composite terrane (Fig. 3). Between the two, and resting on both, lies the Cook Inlet forearc basin. The modern forearc basin had an ancestry in the Triassic, Jurassic, and parts of the Cretaceous when it received many kilometers of sediment from the nearby magmatic arc. The early Tertiary history of this basin bears on the ridge subduction hypothesis (Trop et al., this volume, Chapter 4). The active volcanoes of the modern arc are built largely on basement of the Wrangellia composite terrane, which includes arc batholiths and associated volcanic and volcaniclastic rocks of Jurassic, Cretaceous, and early Tertiary age. The inboard suture of the Wrangellia composite terrane is marked by a belt of deformed Jurassic-Cretaceous flysch, host to a suite of 59–55 Ma granitic plutons that will be mentioned in a later section on possible inboard effects of the slab window. The complex region between the Alaska Range and Brooks Range (Fig. 1), underlain largely by the Yukon-Tanana continental margin terrane, is of only peripheral interest to the present study. In northern Alaska, the Brooks Range orogen records a Jurassic to Early Cretaceous collision between the Yukon-Koyukuk magmatic arc and a south-facing (present coordinates) passive margin of the Arctic Alaska terrane. Tectonic transport was to the north and the resulting orogenic load formed a foreland basin on Alaska's North Slope (Fig. 1). The Alaskan terrane collage is cut by margin-parallel strike-slip faults such as the Border Ranges, Denali, and Tintina (Fig. 1). As will be discussed, the sense, amount, and timing of motion bears on correlations between events in the Alaskan interior and those in the Chugach–Prince William terrane.

The Chugach–Prince William accretionary prism is subdivided into belts of accreted ocean-floor rocks that young in a seaward direction. The most landward belt consists of high-pressure metamorphic rocks (Fig. 3) that were metamorphosed during the Early Jurassic, as summarized, for example, by Dusel-Bacon et al. (1993). The next belt is an argillite-matrix melange containing blocks and fault slices of Triassic to middle Cretaceous chert and basalt, undated graywacke, rare Permian limestone, and a few Triassic-Jurassic ultramafic-mafic complexes (Uyak Complex, McHugh Complex, and Kelp Bay Group; Connelly, 1978; Bradley and Kusky, 1992; Decker, 1980). Small near-trench plutons and numerous dikes intrude these rocks. The next outboard belt contains Upper Cretaceous flysch that has been assigned to the Shumagin Formation, Kodiak Formation, Valdez Group, and part of the Sitka Graywacke (Moore, 1973; Nilsen and Moore, 1979; Nilsen and Zuffa, 1982; Decker, 1980). The biggest near-trench plutons and largest areas of high-temperature, *low*-pressure metamorphism occur in the Upper Cretaceous flysch belt. In Prince William Sound, mafic volcanic rocks are interbedded with flysch assigned to the Valdez Group. Farther outboard lie belts of flysch assigned to the Ghost Rocks Formation and Orca Group (Moore et al., 1983; Moore and Allwardt, 1980; Helwig and

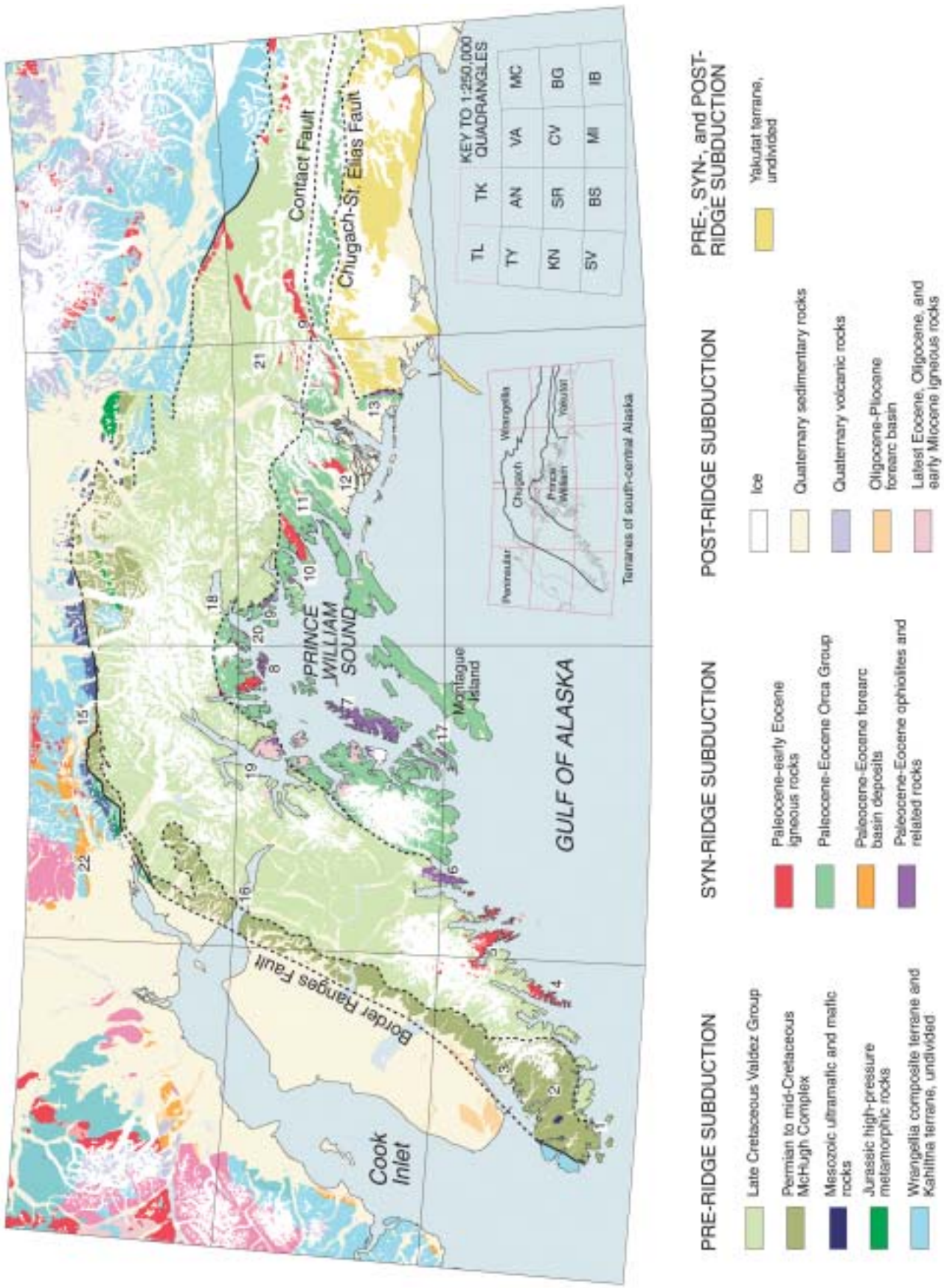

Figure 3. Geologic map of south-central Alaska showing belts of accreted rocks, near-trench igneous rocks, and localities mentioned in text. Abbreviations for quadrangles: AN—Anchorage; BG—Bering Glacier; BS—Blying Sound; CV—Cordova; IB—Icy Bay; KN—Kenai; MC—McCarthy; MI—Middleton Island; SR—Seward; SV—Seldovia; TK—Talkeetna Mountains; TL—Talkeetna; TY—Tyonek; VA—Valdez. (Talkeetna and Talkeetna Mountains quadrangles are outside the map area.)

Emmet, 1981). These units include mafic and ultramafic rocks that, we will argue, formed near the trench-ridge-trench triple junction. Penetrative deformation and regional metamorphism occurred in the accretionary prism during and shortly after subduction-accretion in the Jurassic, Cretaceous, and Paleocene (Dusel-Bacon et al., 1993). Near-trench plutons were emplaced into the accretionary prism after this deformation. More deep-sea turbidites (Eocene Sitkalidak Formation and the outboard part of the Orca Group; Moore and Allwardt, 1980; Helwig and Emmet, 1981) occur outboard of the Sanak-Baranof belt; these younger turbidites are not cut by the plutons, and were deposited and accreted after near-trench magmatism.

The Yakutat terrane, which occupies a belt along the coast where the Alaskan panhandle joins the mainland (Figs. 2 and 3), is regarded as a segment of the Chugach–Prince William terrane, now located some 600 km north of its original position (Plafker et al., 1994). Like the Chugach–Prince William terrane, the Yakutat includes Mesozoic melange and flysch, and Tertiary near-trench plutons (Plafker et al., 1994). A 3 km thick succession of late Paleocene to Eocene marine clastic rocks, basalt, and minor coal, which has no obvious counterpart in the Chugach–Prince William terrane, spans the age of near-trench magmatism—but connections between particular rock units and tectonic regime have not yet been studied.

NEAR-TRENCH INTRUSIVE ROCKS

Near-trench intrusive rocks along the Gulf of Alaska margin (Fig. 2) are of two broad age groups: Paleocene to early Eocene, and latest Eocene to early Miocene. The latter present an intriguing problem, but are younger than events of interest here. The Paleocene to early Eocene plutons include granodiorite, granite, tonalite, and gabbro (Hudson et al., 1979; Hudson, 1983). Swarms of basaltic to rhyolitic dikes, known or inferred to be of the same range of ages as the Paleocene to early Eocene plutons, have been mapped along some sectors of the margin.

The mapped limits of the Sanak-Baranof plutonic belt and the Chugach–Prince William accretionary prism are nearly identical. To the west of Sanak Island, any offshore continuation of the near-trench intrusive belt would presumably follow the Beringian margin (Fig. 1) where a pre-Eocene accretionary prism is inferred in the subsurface (Worrall, 1991). The Sanak-Baranof belt is not recognized to the southeast of Baranof Island, but, subject to restoration of 600 km of margin-parallel dextral displacement, the near-trench plutons of the Yakutat terrane would appear to represent the former southeastward continuation of the belt.

Geochronology

Near-trench magmatism progressed from west to east. This is shown in two plots, one for U/Pb and $^{40}Ar/^{39}Ar$ ages and another for conventional K/Ar and Rb/Sr isochron ages (Fig. 4). The conventional K/Ar data (Fig. 4B) have considerable scatter and large error bars, and the black-box nature of the method sometimes makes it difficult if not impossible to tell a "good" date from one that reflects excess argon, partial argon loss, or complete resetting. Two decades ago, when only K/Ar and Rb/Sr data were available, some researchers held that the near-trench intrusives fell into two age groups, ca. 60 Ma in the west and ca. 50 Ma in the east (e.g., Hudson et al., 1979). Others (e.g., Helwig and Emmet, 1981; Moore et al., 1983) interpreted a more gradual younging trend. Following W. Clendenen (1989, written commun.), Bradley et al. (1993) compiled available geochronology and, by means of early versions of Figures 4A and 4B, showed a clear west-to-east younging trend. Since 1993, new $^{40}Ar/^{39}Ar$ and U/Pb dating has confirmed and refined the age progression (Fig. 4A) (Bradley et al., 1993, 2000; Haeussler et al., 1995). Most convincing is the trend shown by the concordant U/Pb TIMS data from zircon and monazite—the least equivocal way to date granitic rocks of this age. These were deliberately shown with the boldest symbols in Figure 4A. The other data in Figure 4A show the same overall west-to-east younging trend, but are not as bombproof—the discordant U/Pb ages because they rest on a judgment of whether inheritance or lead loss was responsible for discordance, and the $^{40}Ar/^{39}Ar$ ages because they date cooling rather than intrusion.

The age-distance plots in Figure 4 show several other tectonically significant features. (1) Other fields. Most of the conventional K/Ar data shown (Fig. 4B) clearly correspond to the diachronous cluster of U/Pb and $^{40}Ar/^{39}Ar$ data (Fig. 4A)—the "main Sanak-Baranof trend" as used below. Some of the K/Ar ages, however require other explanations. Fields 2 and 3 are younger than the main Sanak-Baranof trend, and are seen in both Figures 4A and 4B. Field 2 corresponds to the late Eocene to Oligocene plutons of Prince William Sound. Field 3 likely includes a combination of emplacement ages in the range 35–45 Ma, and reset or cooling ages of older plutons. Field 1, older than the main Sanak-Baranof trend, is a group of conventional K/Ar amphibole ages suspected of reflecting excess argon (Onstott et al., 1989). Bradley et al. (1993) provided some additional discussion of these fields. (2) Onset of magmatism. Magmatism began ca. 61 Ma on Sanak Island but not until 51 Ma on Baranof Island, some 2200 km along strike to the east (Fig. 4). The 61 Ma age quoted here for the onset of magmatism at the western end of the belt is based on a new concordant U/Pb zircon age of the Shumagin pluton (Bradley et al., 2000) and is younger than the 63–66 Ma age range quoted by Bradley et al. (1993), which was based on the K/Ar and Rb/Sr ages shown in Figure 4B. The 51 Ma age quoted here for the *onset* of magmatism at the eastern end of the belt (Bradley et al., 1993) is based on one new concordant U/Pb and two new $^{40}Ar/^{39}Ar$ plateau ages, and is older than the 50 Ma age quoted by Bradley et al. (1993). (3) Duration of magmatism at a given place. At face value, the dates in Figure 4A would seem to suggest that magmatism locally spanned 3–5 million years, at least along certain sectors of the margin. Conversely, near-trench magmatism would appear to have taken place simultaneously along a considerable length (~500 km) of continental margin.

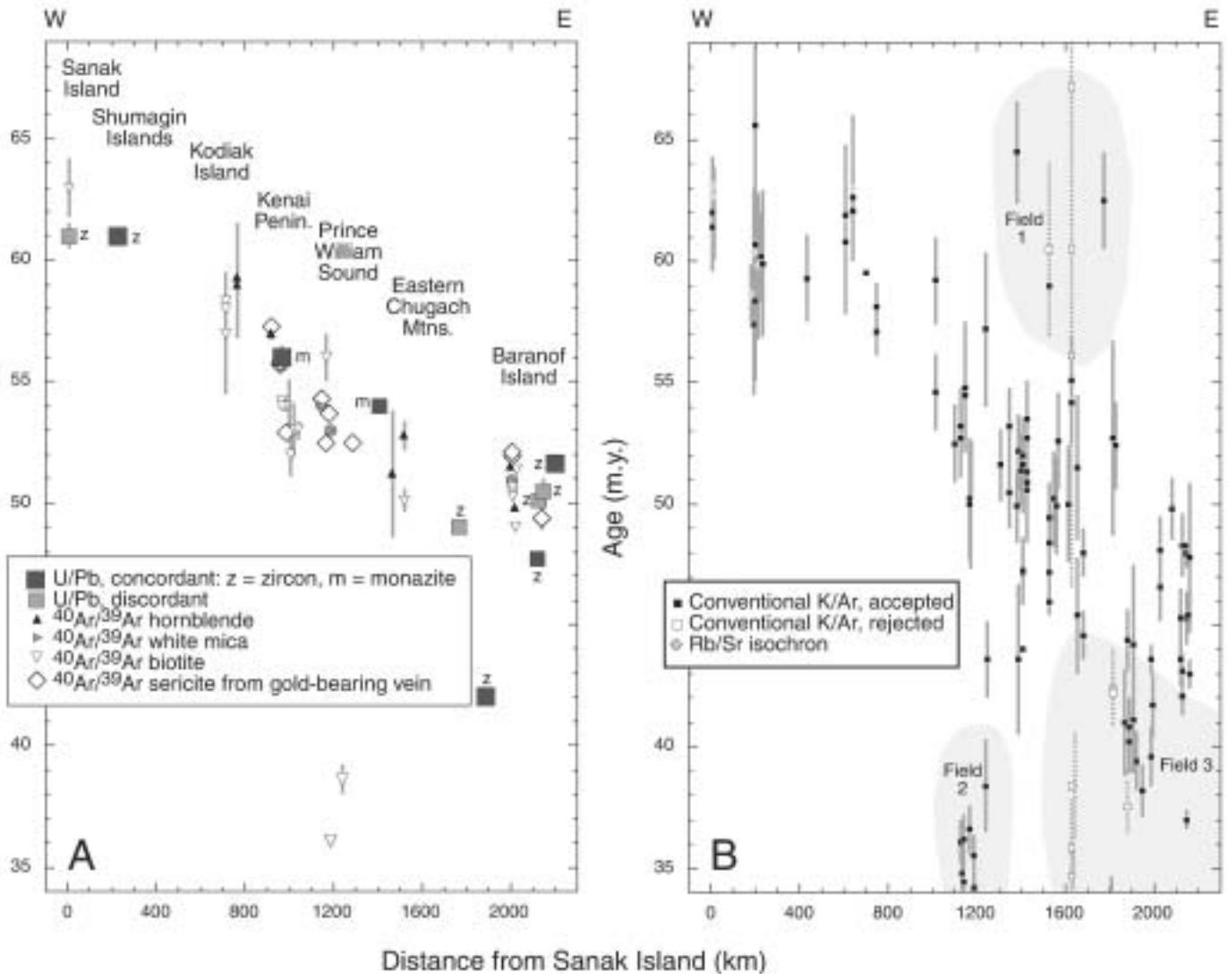

Figure 4. Isotopic ages of near-trench intrusive rocks of the Sanak-Baranof belt, plotted against distance along strike. Distances along the x-axis were measured from Sanak Island on Beikman's (1980) geologic map of Alaska; the map projection was responsible for errors up to about +5% in some cases. Data in this plot are mainly from the tabulation by Bradley et al. (1993) and two sequential updates, by Haeussler et al. (1995) and by Bradley et al. (2000). Table 1 summarizes new results since the latter paper went to press, and was current as of September 2001. Other papers in this volume may contain new dates that are not plotted here or listed in Table 1. A: U/Pb and $^{40}Ar/^{39}Ar$ ages. Short error bars are obscured behind the symbols for most dates. B: Conventional K/Ar and Rb/Sr isochron ages. "Rejected" K/Ar ages are shown for the sake of completeness, but have errors >10% or are significantly younger than other K/Ar ages from the same sample.

Only on Baranof Island, however, has a significant (~4 m.y.) age span been confirmed by concordant U/Pb ages. Some of the apparent age span is probably an artifact of cooling ages.

Petrology and Geochemistry

The predominant plutonic rock of the Sanak-Baranof belt is granodiorite (Fig. 5). Some plutons also include granite, tonalite, and quartz diorite phases (Fig. 5), which mainly differ from the granodiorites in the proportion of K-feldspar. Tonalite and quartz diorite are more common in the eastern than the central or western parts of the belt. All of these show calc-alkaline affinities (Fig. 6). Point-count data from a variety of plutons indicate plagioclase, quartz, biotite and K-feldspar as the major minerals listed in order of decreasing abundance. Hornblende is present in a few plutons, muscovite in others. Zircon and apatite appear to be ubiquitous; monazite has been noted in two plutons. Magmatic andalusite occurs in one pluton in the Chugach metamorphic complex (J. Sisson, 2001, written commun.). The Nuka pluton (Fig. 3) appears to be the source of corundum in pan concentrates from a number of drainages entirely within the pluton (D. Tripp, U.S. Geological Survey, 1993, written commun.). Kyanite xenocrysts, discussed later, have been reported from at least five plutons (Hill et al., 1981; Kusky et al., this volume, Chapter 12).

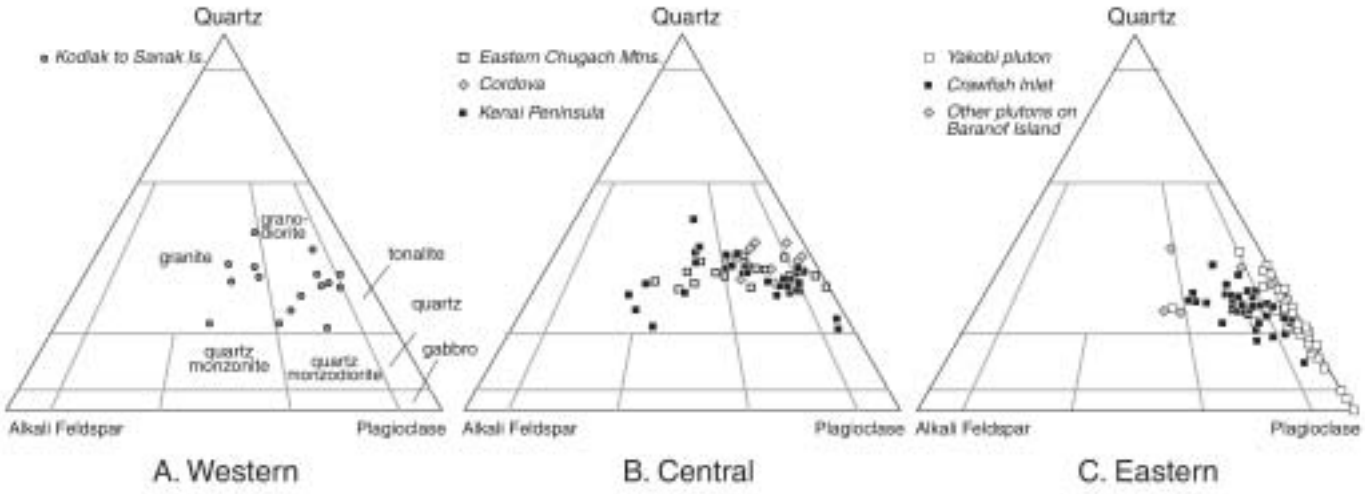

Figure 5. Ternary diagrams of point counts of plutonic rocks from three sectors of the Sanak-Baranof belt. Rock classification fields from Streckeisen (1973). Data are from Hudson et al. (1979), Tysdal and Case (1979), Reifenstuhl (1986), and our data from Seldovia quadrangle, Prince William Sound, and Sitka quadrangles.

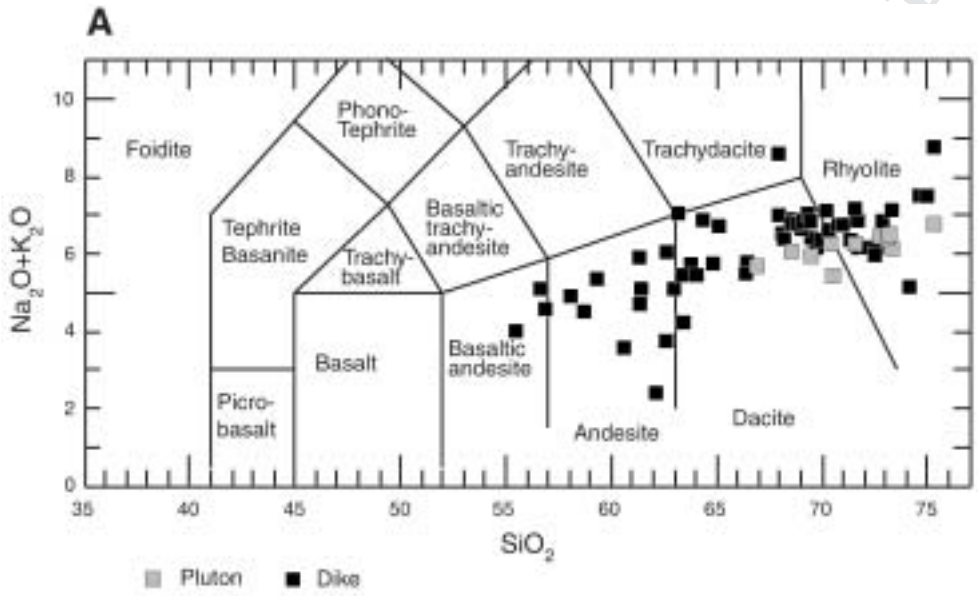

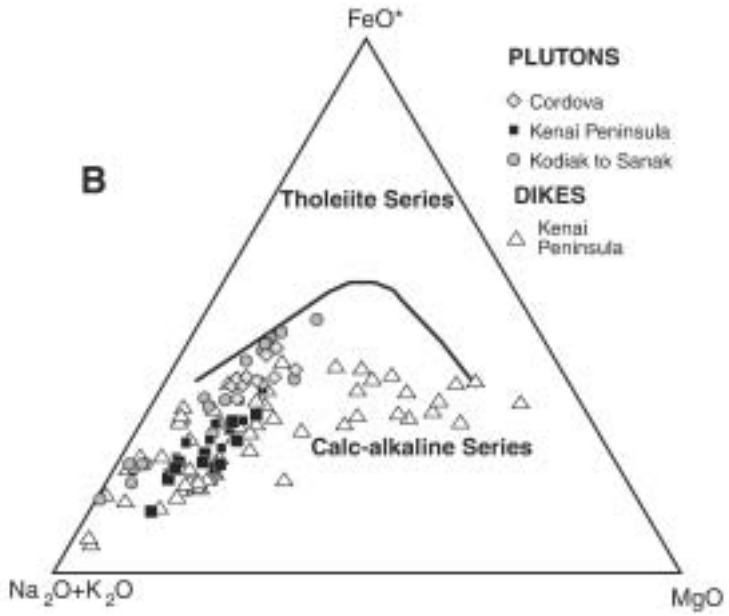

Figure 6. A: $K_2O + Na_2O$ plotted against SiO_2 for the least altered dikes and plutonic rocks from the Kenai Peninsula. Petrographic fields are from LeBas et al. (1986). B: AFM ternary diagram showing calc-alkaline affinity of the same samples. A—alkalis as $K_2O + Na_2O$; F—iron as $FeO + Fe_2O_3$; M—magnesium as MgO.

Gabbroic plutons have been described from as far west as Kodiak (Moore et al., 1983), but appear to be much more abundant in the eastern half of the Sanak-Baranof belt. Until very recently, the geochronological basis for including these mafic plutons in the Sanak-Baranof belt was problematic and merits a brief digression. Conventional K/Ar ages on these rocks range from 19 to 64 Ma (Bradley et al., 1993); none, however fall exactly within the 61–50 Ma range that has been established for Sanak-Baranof magmatism by modern geochronological methods. When Bradley et al. compiled the available geochronology in 1993, the most compelling evidence for including any of the mafic plutons in the Sanak-Baranof belt was from the Rude River pluton (location 10, Fig. 3), which includes a gabbroic phase that had yielded a conventional K/Ar hornblende age of 64.5 Ma (probably too old due to excess argon), and a granodiorite phase that had yielded a K/Ar biotite age of 52.3 Ma. Better evidence is now available. Gabbroic bodies on Yakobi and Chichagof Islands (Fig. 2) grade into and are comagmatic with tonalite (Himmelberg et al., 1987) that recently has yielded $^{40}Ar/^{39}Ar$ biotite ages of 50.3 and 50.5 Ma (Table 1). In this volume (Chapter 13), Sisson et al. report a $^{40}Ar/^{39}Ar$ hornblende plateau age of 53.8 ± 0.4 Ma from a diorite in the Yakutat terrane near Yakutat. Himmelberg et al. (1987, their Figs. 3–5) showed that the mafic rocks on Yakobi and Chichagof Islands range from hornblende pyroxenite to hornblende-pyroxene gabbronorite to quartz-bearing gabbronorite and gabbronorite. Local magmatic sulfide deposits (e.g., Bohemia Basin), which presumably formed from an immiscible sulfide melt in the silicate magma, contain pyrite, chalcopyrite, and pentlandite (Himmelberg et al., 1987). Another well-studied pluton, associated with the much larger Brady Glacier magmatic sulfide deposit, is the funnel-shaped La Perouse layered mafic-ultramafic intrusion (Fig. 2) (Loney and Himmelberg, 1983). Unfortunately, it has not been reliably dated, having yielded a number of difficult-to-interpret K/Ar and $^{40}Ar/^{39}Ar$ ages on biotite and hornblende ranging from 44 to 28 Ma (Bradley et al., 1993).

Dikes of the Sanak-Baranof belt have been studied most thoroughly in the Seldovia quadrangle (Fig. 3) (Bradley et al., 1999; Lytwyn et al., 2000). Almost all are dacite, rhyolite, or andesite (Fig. 6A). The rhyolite dikes are porphyritic, containing 10–20% phenocrysts (.5 to 2 mm) in a very fine groundmass. Phenocrysts include plagioclase ± resorbed quartz ± biotite. The microcrystalline to granular groundmass has plagioclase > quartz > potassium feldspar, and secondary white mica and locally, minor epidote. The dacite dikes, where porphyritic, contain phenocrysts of plagioclase (commonly zoned), lesser to no mafic minerals (altered biotite and locally amphibole), and rarely potassium feldspar and garnet. Groundmass consists of plagioclase > quartz > potassium feldspar, and locally biotite altered to chlorite. Secondary white mica and calcite are ubiquitous. The andesite dikes are primarily fine-grained seriate texture. Locally, the andesite is porphyritic, containing up to 10% phenocrysts of brown hornblende in a groundmass of plagioclase, brown hornblende, chlorite after an unknown mafic mineral, minor quartz, and little to no potassium feldspar. Hornblende is locally altered to actinolite + chlorite. Some samples have secondary white mica and prehnite. The basaltic andesite is generally fine-grained seriate in texture consisting of plagioclase, clinopyroxene, and lesser quartz. The clinopyroxene is partly replaced by brown hornblende and later chlorite. Secondary prehnite, sphene, and minor epidote occur between grains; calcite alteration is present locally. Alteration is pervasive, as might be expected of dikes emplaced into a submarine accretionary prism.

The dikes are correlated on geochronological grounds with the Sanak-Baranof plutons. A dacite dike yielded a $^{40}Ar/^{39}Ar$ hornblende age of 57.2 ± 0.8 Ma (Bradley et al., 2000); an altered, weakly mineralized dike yielded a $^{40}Ar/^{39}Ar$ sericite age of 57.3 ± 0.1 Ma (Haeussler et al., 1995). Comparable ages have been obtained from nearby plutons and all of these dates fall on the Sanak-Baranof age trend (Fig. 4). One other dike from the Seldovia quadrangle yielded a surprisingly old $^{40}Ar/^{39}Ar$ hornblende age of 115.0 ± 1.7 Ma (Bradley et al., 2000) (location 2, Fig. 3). This hornblende-phyric basaltic andesite, which cuts the McHugh Complex, is petrographically distinct—but its existence does make us suspect that at least a few other dikes in the McHugh Complex are older than the Sanak-Baranof intrusive rocks.

Major- and trace-element geochemical data have been reported for a number of plutons and dikes in the Sanak-Baranof belt (e.g., Hill et al., 1981; Barker et al., 1992; Lytwyn et al., 2000). Probably the most comprehensive data set available—11 plutons and 74 dikes—is from the Seldovia quadrangle (analytical data are in the Appendix[1]). Although the dikes as a group have a much wider range of SiO_2 than the plutons, major- and trace-element data overlap. Both plot in the calc-alkaline field of an AFM diagram (Fig. 6B). Chondrite-normalized REE abundances vary with silica composition (Fig. 7A–E). The least-altered mafic rock, a basaltic andesite, has a flat, MORB-like pattern; the intermediate and siliceous dikes and the granodiorite plutons are enriched in light REE. Some rhyolites and granites show a pronounced negative Eu anomaly. Trace element spidergrams from the same samples (Fig. 7F–J), normalized to chondrite after Sun (1980), show similar variations with silica composition. The basaltic andesite sample lacks any strong anomalies and broadly resembles the E-MORB pattern illustrated by Sun and McDonough (1989). The intermediate and siliceous dikes and the granodiorite plutons show negative anomalies in Ta, P, and Ti and a strong positive Pb anomaly. Mafic dikes from the Seldovia area are transdicriminant on various tectonic discriminant plots (Lytwyn et al., 2000).

Recent workers have differed only in detail on the petrogenesis of the Sanak-Baranof intrusives. On the basis of Sr-

[1]GSA Data Repository item 2003XXX, Appendix 1, geochemical analytical data for near-trench intrusive rocks, Seldovia quadrangle, Alaska (Table DR1, "Geologic signature of early Tertiary ridge subduction in Alaska), is available on request from Documents Secretary, GSA, P.O. Box 9140, Boulder, CO 80301-9140, USA, editing@geosociety.org, at www.geosociety.org/pubs/ft2003.htm, or on the CD-ROM accompanying this volume.

TABLE 1. RECENTLY DETERMINED ISOTOPIC AGES OF INTRUSIVE ROCKS FROM THE SANAK-BARANOF BELT

Igneous body	Quad	Field number or location	Latitude (N.)	Longitude (W.)	Age (Ma)	Error (m.y.)	Method and mineral	Distance from Sanak Island (km)	Reference or geochronologist
Lost Cove pluton	SI	93CH-47	57°51'33"	136°24'36"	51.5	0.1	$^{40}Ar/^{39}Ar$ hornblende	2003	C. Taylor, R. Goldfarb, L. Snee, written communication, 2001
Lost Cove pluton	SI	93CH-47	57°51'33"	136°24'36"	52.0	0.1	$^{40}Ar/^{39}Ar$ biotite	2003	C. Taylor, R. Goldfarb, L. Snee, written communication, 2001
Mirror Harbor pluton	SI	92RG-15	57°46'16"	136°18'12"	50.3	0.1	$^{40}Ar/^{39}Ar$ biotite	2007	Taylor et al. (1994)
Mirror Harbor pluton	SI	92RG-14A	57°46'50"	136°18'10"	50.5	0.1	$^{40}Ar/^{39}Ar$ biotite	2007	Taylor et al. (1994)
Lake Elfendahl pluton	SI	93CH-46	57°50'10"	136°18'05"	50.7	0.1	$^{40}Ar/^{39}Ar$ biotite	2005	C. Taylor, R. Goldfarb, L. Snee, written communication, 2001
Lake Elfendahl pluton	SI	79RB062A	57°49'45"	136°17'05"	50.9	0.1	$^{40}Ar/^{39}Ar$ muscovite	2005	L. Snee & S. Karl, unpublished data
White Sisters–Granite Islands pluton at White Sisters	SI	93CH-29	57°38'00"	136°15'10"	49.0	0.1	$^{40}Ar/^{39}Ar$ biotite	2020	C. Taylor, R. Goldfarb, L. Snee, written communication, 2001
White Sisters–Granite Islands pluton at Outer Rocks	SI	93CH-27B	57°34'12"	136°09'10"	49.8	0.1	$^{40}Ar/^{39}Ar$ hornblende	2022	C. Taylor, R. Goldfarb, L. Snee, written communication, 2001
White Sisters–Granite Islands pluton at Granite Islands	SI	D152a	57°35'58"	136°11'51"	46.6	1.4	K/Ar	2025	Decker (1980)
Khaz Bay pluton	SI	D281a	57°34'07"	136°04'40"	48.1	1.4	K/Ar	2030	Decker (1980)
Khaz Bay pluton	SI	92RG-09	57°34'09"	136°04'42"	51.4	0.1	$^{40}Ar/^{39}Ar$ biotite	2030	Taylor et al. (1994)
Crawfish Inlet pluton	PA	99SK121A	56°44'27"	135°04'30"	50.5	0.5	U/Pb zircon	2150	S. Karl, P. Haeussler, R. Friedman, unpublished data
Redfish Bay pluton	PA	99PH567A	56°19'42"	134°47'48"	51.6	0.3	U/Pb zircon	2198	S. Karl, P. Haeussler, R. Friedman, unpublished data

Note: This summary of the most recent isotopic ages of intrusive rocks from the Sanak-Baranof belt, southern Alaska, is plotted in Figure 4. SI—Sitka 1:250,000 quadrangle. PA—1:250,000 quadrangle. Distance along strike was measured from the western tip of Sanak Island on Beikman's (1980) geologic map of Alaska; the map projection causes some distortion. This table updates the original compilation by Bradley et al. (1993), and the more recent supplements by Haeussler et al. (1995) and Bradley et al. (2000).

isotopes and trace elements, Hill et al. (1981) interpreted the Kodiak, Shumagin, and Sanak granodiorite plutons as the products of mixing between MORB from a subducted spreading center and melted flysch of the overlying accretionary prism. Kyanite and garnet xenocrysts in several of the plutons (Hill et al., 1981) imply that the granodiorite magmas originated at depths of at least 20 km in aluminous metasediments of the accretionary prism. Barker et al. (1992), working with the most complete geochemical and isotopic data set, interpreted three granodiorite plutons near Cordova as the product of partial melting of arc-derived flysch at depth in the accretionary prism. These plutons have the following isotopic compositions: $^{87}Sr/^{86}Sr$ = 0.7051–0.7067, $^{206}Pb/^{204}Pb$ = 19.04–19.20, $^{207}Pb/^{204}Pb$ = 15.60–15.66, $^{208}Pb/^{204}Pb$ = 38.59–38.85, and ε_{Nd} = +2.1 to –3.3—values that overlap with isotopic compositions from the Orca Group flysch and provide evidence that the granodiorites formed by melting of flysch. Barker et al. (1992) suggested that the most likely source of heat, and of mantle melts that formed the gabbroic plutons, was a ridge-transform complex similar to the one presently bounding the Explorer plate off the Cascadia margin. They interpreted dacite dikes in their study area as the products of partial melting of basalts at depth in the accretionary prism. Harris et al. (1996), on the basis of trace-element and Sr- and Nd-isotopic abundances, similarly interpreted felsic dikes in the Chugach metamorphic complex in terms of mixing between melted flysch and a mafic source associated with subduction of the Kula-Farallon ridge. Based on trace elements, Lytwyn et al. (2000) interpreted dikes from the Seldovia quadrangle as representing a spectrum from I-type basalts and andesites to S-type dacites and rhyolites, the more silicic com-

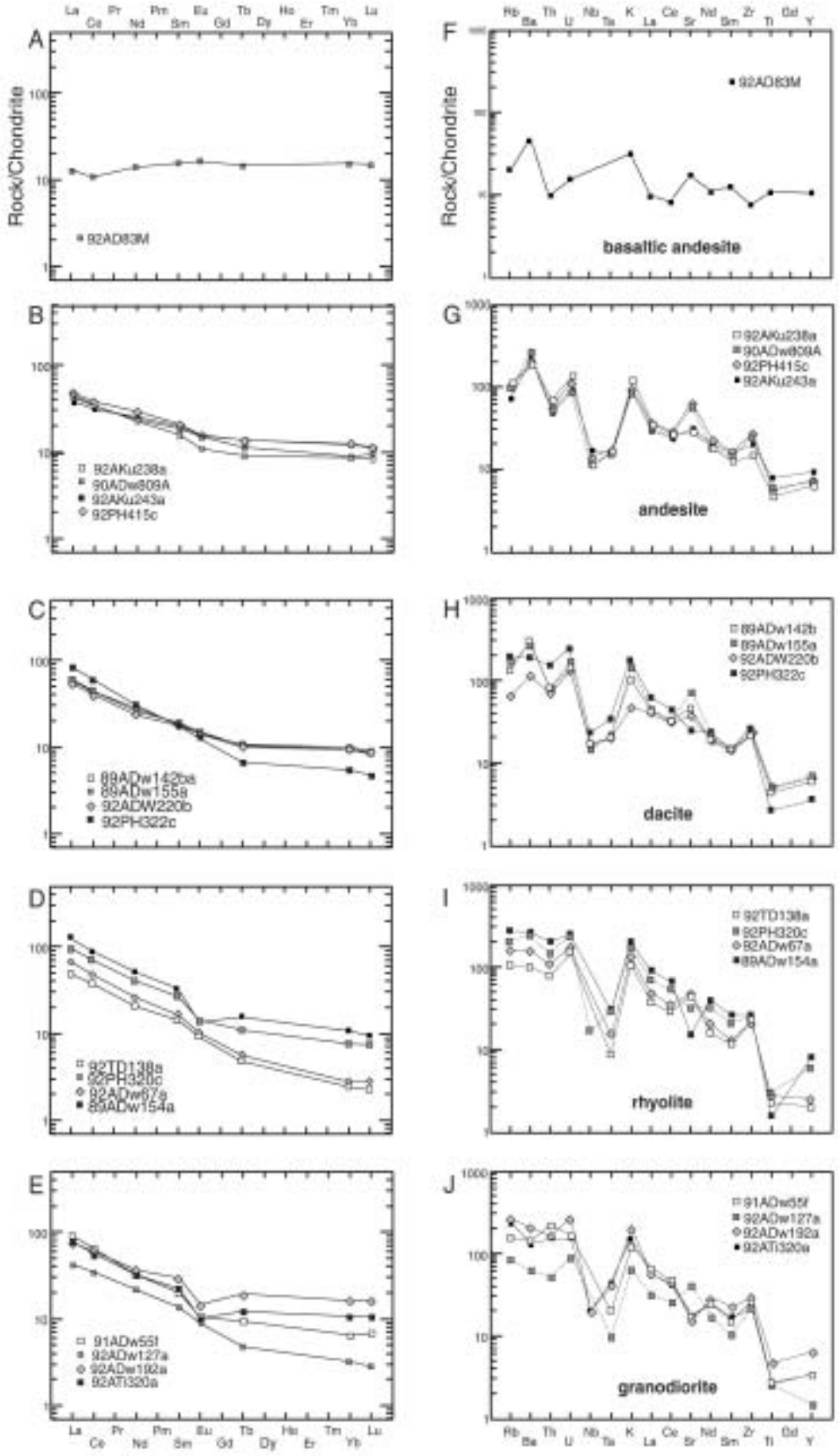

Figure 7. A–E: REE diagrams for dikes and plutons of the Sanak-Baranof belt, Seldovia quadrangle, normalized to chondrite after Sun and McDonough (1989). F–J: Spidergrams of the same samples, normalized to chondrite after Sun (1980). Samples plotted are the least altered representatives of each rock type.

positions reflecting assimilation of sedimentary protoliths at the base of the accretionary prism.

Structure of the Intrusive Rocks

Intrusive bodies of the Sanak-Baranof belt range from dikes to plugs to batholiths. The larger plutons vary in shape from concordant, elongate sill-like bodies (Kodiak batholith) to discordant, irregularly shaped masses (Aialik pluton). The plutons and dikes were intruded after most of the regional deformation, but some penetrative deformation was coeval with magmatism, and some deformation happened even later. In the Seldovia quadrangle, dikes typically crosscut accretion-related structures (Fig. 8C), showing that near-trench magmatism occurred late in the structural sequence. Most are unfoliated, but a few display a weak tectonic foliation. Similarly, the Nuka and Aialik plutons (locations 4 and 5, Fig. 3) are discordant in most places, truncating folds, cleavage, and melange fabrics, which are all attributed to subduction-accretion (Kusky et al., 1997b). The interiors of these plutons are unfoliated but a tectonic foliation is well developed along the Nuka pluton's concordant landward contact (Fig. 8B) (Kusky et al., this volume, Chapter 12). Contact-metamorphic textures in the adjacent Valdez Group provide additional evidence for syn-emplacement deformation (Fig. 9). In the Chugach metamorphic complex (Fig. 2), dikes, sills, and plutons of the Sanak-Baranof belt have been assigned to four generations, of which the second and third were emplaced syntectonically (Pavlis and Sisson, 1995; Harris et al., 1996).

Dikes are abundant in parts of the Sanak-Baranof belt. A regional compilation map of dike orientations (Fig. 10; from Haeussler et al., this volume, Chapter 5) shows several important features. (1) In southeastern Alaska, dikes strike NW, subparallel to the margin. (2) Dikes in the broad hinge area of the southern Alaska orocline have quite uniform strikes of approximately N-S, at a high angle to the margin but at a varying angle with respect to the local structural grain. (3) In the Seldovia quadrangle, dike strikes are roughly E-W, nearly perpendicular to the structural grain. Separate rose diagrams for mafic to intermediate and felsic dikes in Seldovia quadrangle show slightly different orientations. Except in southeastern Alaska, the net effect of dike emplacement was orogen-parallel extension. The cumulative thickness of dikes measured in the Seldovia quadrangle suggests as much as 1% extension due to dike injection alone.

OBDUCTED EARLY TERTIARY OPHIOLITES AND ASSOCIATED MASSIVE SULFIDE DEPOSITS

Geology and Geochemistry

In Prince William Sound and on Kodiak Island, Paleocene to Eocene turbidites are interbedded with mafic pillow lavas and associated subvolcanic diabase and gabbro, an association that has been interpreted in terms of a ridge-trench encounter. Three of the larger belts include pillow lavas, sheeted dikes, and gabbro and are categorized as ophiolites: the Resurrection Peninsula (Nelson et al., 1989; Kusky and Young, 1999), Knight Island (Richter, 1965; Nelson and Nelson, 1993), and Glacier Island ophiolites. Among worldwide examples of ophiolites, these are important because their geologic relations leave little doubt that they formed along an oceanic ridge and *not* in a supra-subduction setting.

The ophiolites are known or inferred to be late Paleocene in age. Plagiogranite from the Resurrection Peninsula ophiolite has been dated at 57 ± 1 Ma (U/Pb zircon; Nelson et al., 1989). The ophiolites at Knight Island and Glacier Island, although undated, are believed to be about the same age as the Resurrection Peninsula body because they are petrologically similar, and crop out amongst the same turbiditic formations in the same strike belt. In the Resurrection Peninsula ophiolite (Tysdal and Case, 1979; Miller, 1984; Nelson et al., 1985; Bol et al., 1992; Kusky and Young, 1999), the pillow lava succession is interbedded with siliciclastic turbidites, suggesting proximity to a continental sediment source during seafloor spreading. An upward transition from thinly bedded to thickly bedded turbidites has been interpreted as a distal-to-proximal facies change recording the migration of the ophiolite toward the continent (Kusky and Young, 1999). The ophiolite is juxtaposed against the Valdez Group along a thrust (Fox Island shear zone of Kusky and Young, 1999) along which a 53.4 ± 0.9 Ma granodiorite pluton was emplaced (Bradley et al., 2000). Thus, only a few million years elapsed between formation of the ophiolite and its incorporation into the accretionary prism. Trace-element abundances from basalts of the Resurrection and Knight Island ophiolites are broadly MORB-like but show some enrichment in incompatible elements (Lytwyn et al., 1997; Nelson and Nelson, 1993; Crowe et al., 1992). These trends can be explained in terms of contamination of normal MORB with sediment in a near-trench setting.

Basalt flows are interbedded with deep-sea fan deposits that have been assigned to the Upper Cretaceous Valdez Group, the Paleocene-Eocene Orca Group, and the Paleocene Ghost Rocks Formation (Fig. 3). Volcanics of the Orca Group (Nelson et al., 1985; Crowe et al., 1992) are thought to be broadly comparable to the ophiolites described above. Volcanics in the Ghost Rocks Formation of Kodiak Island include andesite and basalt flows interbedded with Paleocene turbidites. Volcanic rocks of the Valdez Group (Nelson et al., 1985; Lull and Plafker, 1990) have not been directly dated but if their nominal Late Cretaceous age assignment is indeed correct, they would appear to be older than events of interest here.

Massive Sulfide Deposits

More than 600 massive sulfide deposits and prospects are known from the Chugach–Prince William terrane in Prince William Sound (Crowe et al., 1992). These deposits are inferred to have formed syngenetically along a spreading ridge that at times was sediment-covered, but at other times, or perhaps along cer-

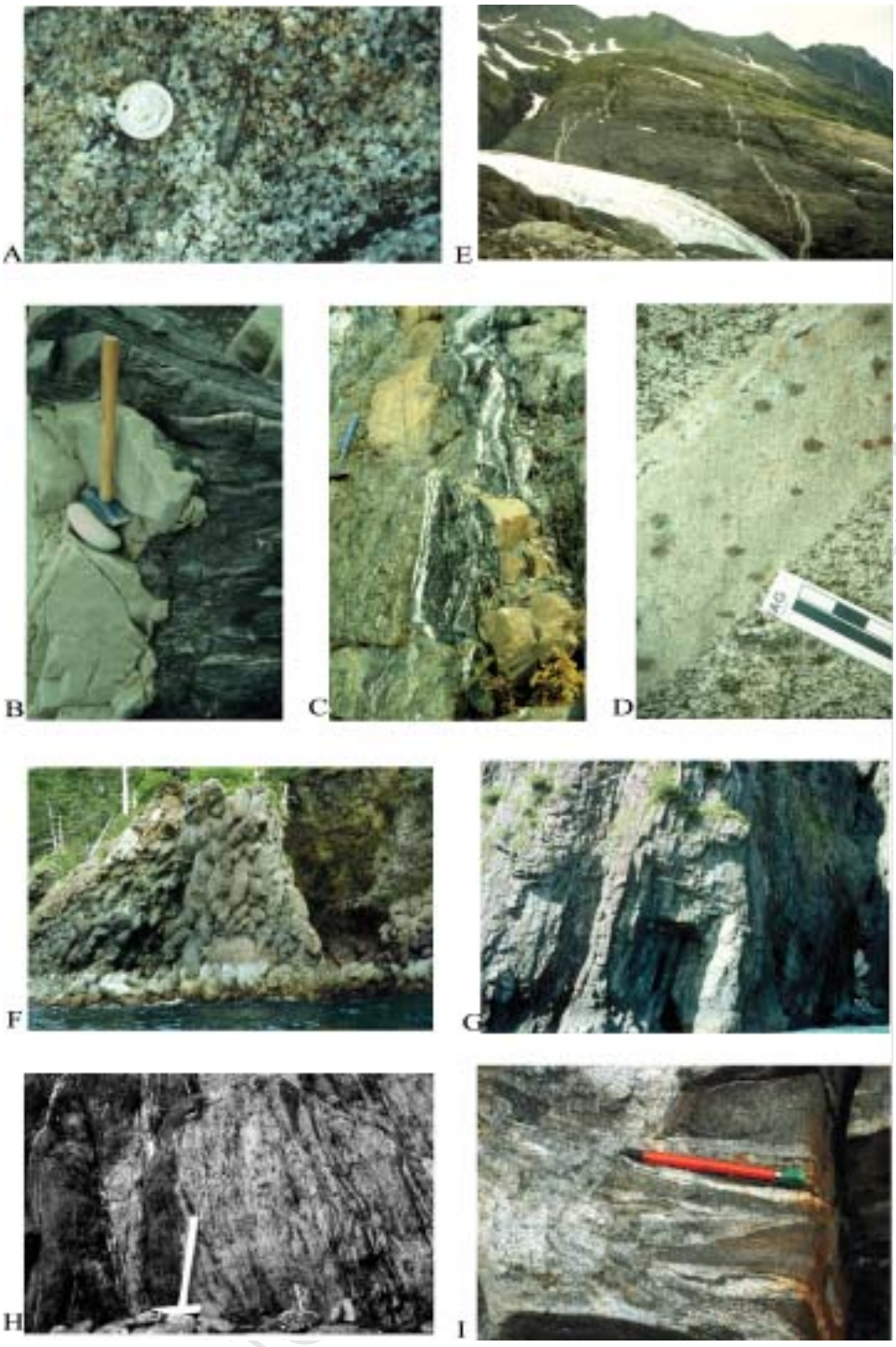

Figure 8. Photographs; all locations are keyed to Figure 3. A: Kyanite xenocryst, Harris Bay, Aialik pluton (location 5). B: Dike cutting melange that marks the McHugh-Valdez contact in the Seldovia quadrangle, showing that most of the accretion-related deformation of the Maastrichtian Valdez Group predated near-trench magmatism (location 1). C: Dike cutting melange fabrics in the McHugh Complex at Grewingk Glacier, Seldovia quadrangle (location 3) (Bradley and Kusky, 1992). D: Foliation cutting both granodiorite of the Aialik pluton and a late-stage aplite dike, showing that the foliation is of tectonic origin (location 5). E: Dikes cutting McHugh Complex, Seldovia quadrangle (location 2). F: Pillow basalt, Resurrection Peninsula ophiolite (location 6). G: Sheeted dikes, Resurrection Peninsula ophiolite (location 6). H: Interbedded basalt and black shale, Orca Group, Prince William Sound (location 20). I: Migmatite (protolith was Valdez Group), Cordova quadrangle (location 21).

tain sectors, was sediment-starved. Crowe et al. (1992) identified two main deposit types: (1) Cyprus-type deposits hosted by pillow basalts, massive basaltic flows, and tuffs (e.g., Rua Cove; deposit location 7, Fig. 3); and (2) Besshi-type deposits hosted by slate and graywacke, which are interbedded with the basaltic rocks (e.g., Ellamar and Beatson deposits; locations 9 and 17, Fig. 3). The largest deposits, up to 5 million tons, are sediment-hosted. Sulfide assemblages typically include pyrite + arsenopyrite + pyrrhotite + chalcopyrite ± sphalerite. Fluid inclusions indicate temperatures of 170–290 °C, consistent with mineralization in sea-floor hydrothermal systems. Sulfur and oxygen isotopes reported by Crowe et al. (1992) are also consistent with submarine mineralization. Mineralization has not been directly dated but most of the deposits, namely those

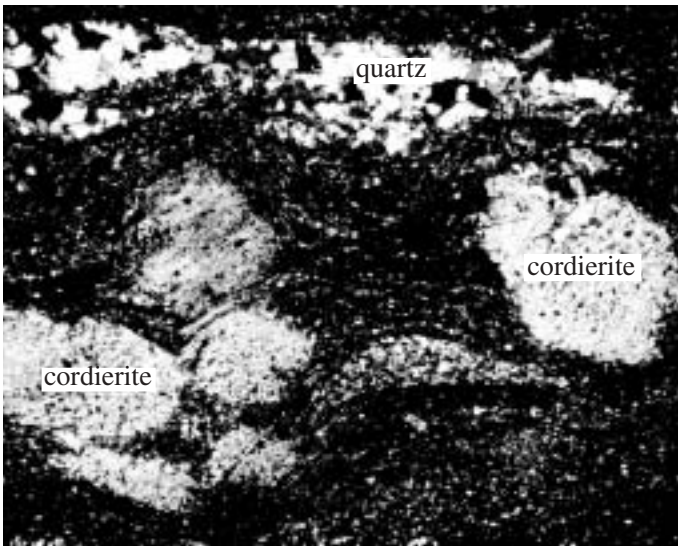

Figure 9. Photomicrograph from the aureole of Nuka pluton showing textural evidence for syntectonic contact metamorphism. Phenocrysts of cordierite surrounded by asymmetric strain shadows of biotite indicate that metamorphism was coeval with deformation. Note weak inclusion trails in cordierite grains that record a layering—either bedding or foliation—that existed prior to contact metamorphism ca. 56 Ma. Regional metamorphic grade is chlorite; cordierite and biotite are found only within the aureoles of the Nuka and allied plutons.

associated with the Knight Island and Glacier Island ophiolites or with volcanic rocks assigned to the Paleocene-Eocene Orca Group, would appear to be roughly the same age as the 57 Ma Resurrection Peninsula ophiolite. The origin of massive sulfide deposits associated with volcanic rocks that have been mapped as part of the Valdez Group remain problematic.

LATE CRETACEOUS–EARLY TERTIARY DEEP-MARINE SEDIMENTATION

Late Cretaceous through Eocene deposition of turbidites that were offscraped or underplated to build the Chugach–Prince William accretionary prism was underway well before, and continued long after, emplacement of the Sanak-Baranof plutons. In the following we will refer to "stage 1" as the ~10 m.y. interval preceding near-trench magmatism at a given location, "stage 2" as the time of near-trench magmatism at that location, and "stage 3" as the ~10 m.y. interval that followed.

Turbidites of stage 1, assigned to the Shumagin and Kodiak Formations, Valdez Group, and Sitka Graywacke, have been interpreted as trench-fill deposits (Moore, 1973; Nilsen and Zuffa, 1982). The Maastrichtian fossil age of these deposits shows that they were deposited 4 to 11 million years before the onset of near-trench magmatism at the western end of the

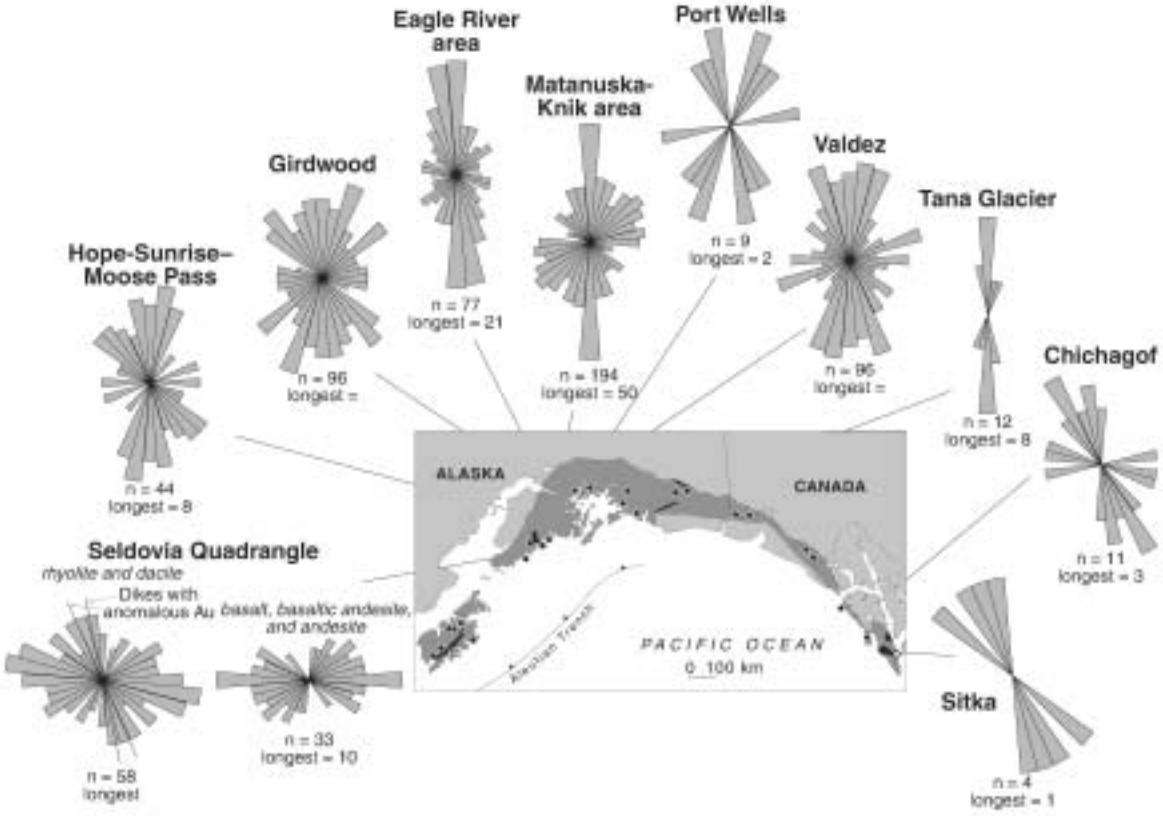

Figure 10. Map showing the strike of dikes in the Sanak-Baranof belt (from Haeussler et al., this volume).

belt. Paleoflow was along the trench axis, mainly toward the western end of the belt (Moore, 1973; Nilsen and Moore, 1979) (Fig. 11).

Sedimentary rocks that are interbedded with volcanic rocks in the Orca Group, the Knight Island and Resurrection Peninsula ophiolites, and the Ghost Rocks Formation correspond to stage 2. Paleocurrent data from the Ghost Rocks Formation indicate turbidity flows toward virtually every point of the compass, in contrast with strong axial paleocurrents of the slightly older Kodiak Formation (Nilsen and Moore, 1979). Some paleocurrent data are also available for the Orca Group (Winkler, 1976), which show flow directions toward the north, west, and south, but not toward the east.

Accreted sedimentary rocks related to stage 3 lie immediately outboard of the Sanak-Baranof near-trench intrusives, the ophiolites, and the volcanic rocks. They are interpreted as closely post-dating the near-trench magmatism episode. On Kodiak Island and adjacent islands, Eocene deep-sea turbidites of this outboard belt have been named the Sitkalidak Formation. Paleocurrent directions reported by Nilsen and Moore (1979) are predominantly toward the southeast (i.e., seaward, perpendicular to the margin).

Sandstone compositions show progressive changes through the time interval of interest, as well as some anomalies corresponding to stage 2 (Fig. 12). In Prince William Sound (Dumoulin, 1987, 1988) sandstones of Stage 1 (Valdez Group and inboard part of the Orca Group) contain abundant volcanic lithic clasts, locally abundant grains of pyroxene and amphibole, and little quartz. They were derived from a progressively unroofing magmatic arc with increasing input from subduction-complex sources through time. Similar compositions have been reported for the Kodiak Formation to the west, and the Sitka Graywacke to the east (e.g., Zuffa et al., 1980). Stage 2 sandstones interbedded with volcanic rocks (locations 6, 7, and 8, Fig. 3) are richer in feldspar and quartz and generally finer grained and better sorted than sandstones in adjacent areas. These differences could be due to barrier effects of local topography. Stage 3 sandstones of the Orca Group on Montague Island (Fig. 3) and the Ragged Mountain area (location 13, Fig. 3) are relatively rich in quartz and sedimentary lithic clasts and correlate well with the Sitkalidak Formation on Kodiak Island to the west (Nilsen and Moore, 1979; Moore et al., 1983). Provenance of these younger rocks reflects increased contributions from subduction complex sources and waning input from a magmatic arc.

GOLD VEINS AND HYDROTHERMAL FLUID-FLOW IN THE ACCRETIONARY PRISM

The Chugach–Prince William terrane is host to dozens of small turbidite-hosted lode-gold deposits. Similarities in structural setting, vein mineralogy, alteration assemblages, stable isotope geochemistry, and fluid inclusion *P-T-X* data for a distance of >1000 km along the continental margin suggest a common origin for these deposits (Goldfarb et al., 1986, 1997). In south-central Alaska, most of the deposits are hosted by rocks of the Valdez Group or the landward part of the Orca Group. In southeastern Alaska, the gold deposits are hosted by the Sitka Graywacke, and by older metamorphic and igneous rocks of the Wrangellia composite terrane within about 5–10 km of the Border Ranges fault system. Many occupy faults, as discussed under the next heading. $^{40}Ar/^{39}Ar$ ages on micas from ten of the gold veins fall along the same age trend as the Sanak-Baranof plutons (Haeussler et al., 1995) (Fig. 4A), requiring a common tectonic setting for magmatism and the regional hydrothermal event.

The gold-bearing veins throughout the Alaskan margin are typically discordant, steeply dipping, high-grade (many 30 g/t Au), and relatively small. The quartz veins contain gold, arsenopyrite, pyrite, and hydrothermal muscovite/sericite. The small size of vein systems suggests that, on the scale of the accretionary prism as a whole, fluid flow was relatively diffuse. The most important producers in south-central Alaska were the Cliff mine (location 18, Fig. 3), which yielded about 1.5 tonnes Au from ore averaging 53 g/t, and the Granite mine (location 19, Fig. 3), which yielded about 0.75 tonnes Au. None of the other small mines in south-central Alaska yielded more than 200,000 g Au. In contrast, the Chichagof/Hirst-Chichagof vein systems in southeastern Alaska contain about 30 tonnes Au (production plus reserves) from ore averaging slightly more than 30 g/t Au. These larger, more productive veins indicate a more voluminous concentration of hydrothermal fluid. Goldfarb et al. (1997) suggested that the onset of transcurrent motion along the southern part of the Border Ranges fault system may have favored establishment of a large second-order fault system that was capable of the more extensive fluid focussing.

The gold deposits are regionally restricted to areas of greenschist facies metamorphic rocks and are only rarely present in lower- or higher-grade metamorphic rocks (Goldfarb et al., 1986, 1997). $\delta^{18}O$ values for quartz from more than 30 deposits range between 13 and 17.5‰; fluid-inclusion microthermometry suggests that veins were deposited from low-salinity aqueous-dominant fluids containing about 5–10 mol% gas at 210–360 °C and 100–300 MPa (1–3 kbar). Quantitative mass spectrometry indicates that the non-aqueous volatiles in the fluids include CO_2, CH_4, N_2, and H_2S. These data are together interpreted to indicate that vein-forming fluids were produced from devolatilization reactions within the previously accreted flysch. Whereas quartz veins (and thus fluid flow) are present throughout the Chugach–Prince William terrane, the restriction of most gold and arsenopyrite to veins in greenschist regions is consistent with desulfidization reactions predominating in these moderate *P-T* regions (e.g., Ferry, 1981). The H_2S made available to crustal fluids during conversion of sedimentary pyrite to pyrrhotite is critical for complexing gold and arsenic in hydrothermal solutions. The H_2S is additionally likely to complex mercury, and transport it into relatively low-*T* crustal regimes. Cinnabar, which has been found in pan concentrates in many drainages in the Seldovia quadrangle (Fig. 2), probably was derived from some of the most shallowly emplaced vein systems.

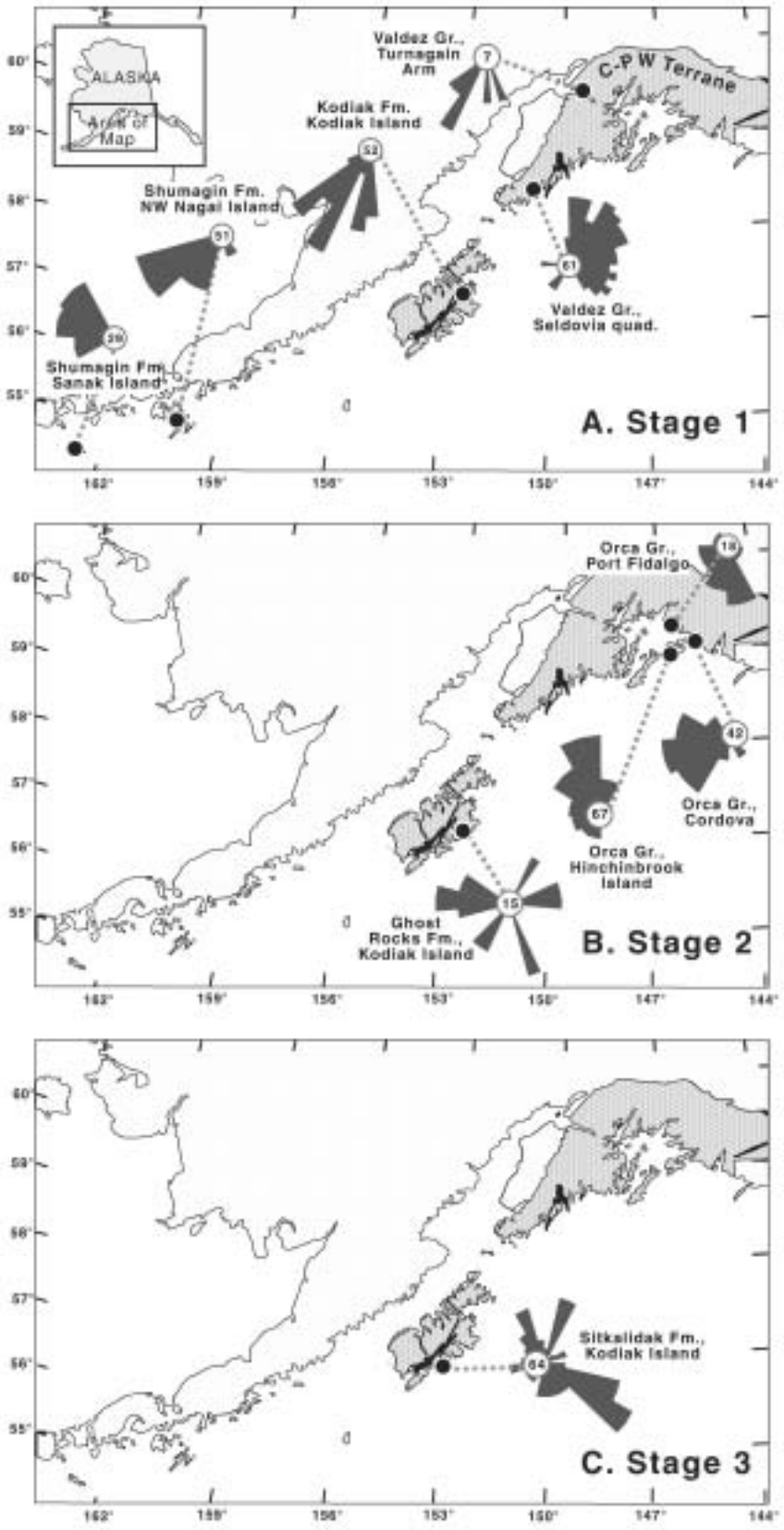

Figure 11. Map of the central portion of the Chugach–Prince William terrane, showing paleocurrent directions from unimodal indicators, mainly turbidite cross laminae and flute casts. A: Stage 1, before near-trench magmatism. B: Stage 2, during near-trench magmatism. C: Stage 3, after near-trench magmatism. Number in each rose diagram corresponds to number of measurements. Rose diagrams for the Shumagin Formation are from Moore (1973); rose diagrams for the Kodiak, Ghost Rocks, and Sitkalidak Formations are derived from Nilsen and Moore (1979); rose diagrams for the Orca Group are from Winkler (1976); rose diagrams for the Valdez Group are based on new data.

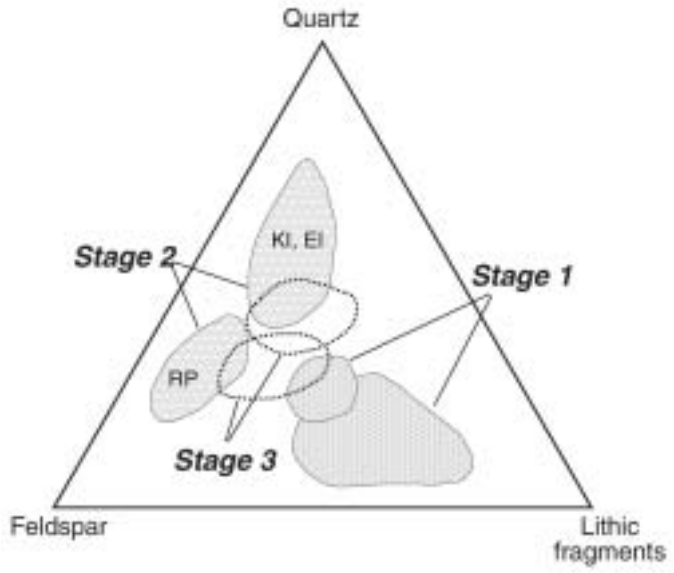

Figure 12. QFL (quartz, feldspar, lithic clasts) diagrams of sandstones deposited before (Stage 1), during (Stage 2), and after (Stage 3) ridge subduction. Abbreviations: RP—Resurrection Peninsula; KI—Knight Island; EI—Ellamar Island. From Dumoulin (1987).

BRITTLE FAULTING

Late brittle faults are common throughout many parts of the Chugach–Prince William terrane, and some of these, at least, were active at the time of near-trench magmatism. Most of the gold-bearing veins described above were developed synkinematically along high-angle faults. $^{40}Ar/^{39}Ar$ sericite ages from these gold lodes thus link fault motion to the time of near-trench magmatism. A structural synthesis of lode-gold deposits along the length of the Chugach–Prince William terrane (Haeussler and Bradley, 1993; Haeussler et al., this volume, Chapter 5) has revealed both common themes and differences in the brittle faulting history. In southeastern Alaska, gold mineralization was coeval with movement on northwest-striking, margin-parallel dextral faults. In south-central Alaska, gold mineralization was associated with normal and strike-slip faults that strike at a high angle to the continental margin and facilitated orogen-parallel extension.

Some of the nonmineralized brittle faults from other parts Chugach–Prince William terrane are likely the same age as those associated with gold. Brittle faults are seen at nearly every outcrop along Turnagain Arm near Anchorage (location 16, Fig. 3); they have been described by Bradley and Kusky (1990) and Kusky et al. (1997a), who recognized: (1) a conjugate set of normal faults that strike perpendicular to the structural grain of accreted rocks; (2) a conjugate set of sinistral and dextral strike-slip faults, the acute bisector of which lies perpendicular to regional strike; and (3) a conjugate set of synthetic and antithetic thrusts, parallel to regional strike. Kusky et al. (1997a) interpreted the three sets as components of a single orthorhombic fault population. Curved slickenlines occur on faults of each type. Populations of minor brittle faults that are broadly similar to those along Turnagain Arm have also been reported from Kodiak Island (Byrne, 1984), Afognak Island (Sample and Moore, 1987), and the Seldovia quadrangle (Bradley and Kusky, 1992), as well as the various gold districts (Haeussler et al., this volume, Chapter 5).

The abundance of brittle faults at many places along the length of the Chugach–Prince William terrane, together with evidence that many, at least, are broadly coeval with Sanak-Baranof magmatism, indicates that the accretionary prism underwent bulk, but non-penetrative deformation at the time of near-trench magmatism. In Prince William Sound and the Kenai Peninsula, brittle faulting resulted in a combination of orogen-perpendicular shortening and orogen-parallel extension. In southeastern Alaska, the structural regime was one of dextral strike slip.

METAMORPHISM OF THE ACCRETIONARY PRISM AND ASSOCIATED DUCTILE DEFORMATION

The Chugach–Prince William terrane, unlike most accretionary prisms, is characterized by anomalous areas of relatively high-temperature, low-pressure metamorphism. Typical background metamorphism, attributed to "normal" processes of subduction-accretion, is the low-grade greenschist facies, which in graywacke is recognized by the assemblage chlorite + epidote ± white mica (Miller, in Goldfarb et al., 1986). Fluid-inclusion studies of synmetamorphic veins on Kodiak Island suggest pressures of 200–300 MPa (2–3 kbar) (Vrolijk, 1987). Chlorite geothermometry from quartz veins in the Chugach metamorphic complex suggests 325–350 °C during the greenschist-facies event (Weinberger and Sisson, this volume, Chapter 9).

The largest area of high-grade rocks is the Chugach metamorphic complex (Hudson and Plafker, 1982; Sisson et al., 1989), a 25 × 180 km belt of amphibolite-facies metamorphism affecting the Valdez Group. Mineral assemblages in the center of the complex include biotite + garnet + staurolite + sillimanite (Sisson et al., 1989). Metamorphic temperatures ranged from 600 to 650 °C and pressures ranged from 250 to 350 MPa (2.5–3.5 kbar), corresponding to depths of 7.5 to 10.5 km (Sisson et al., 1989). The high-temperature metamorphism was superimposed on, and took place after the regional low-grade event.

Smaller areas of anomalous metamorphism, also superimposed on the regional low-grade greenschist facies event, have been mapped on Baranof Island (Loney and Brew, 1987; Karl et al., 1999) (Fig. 2), Prince William Sound (Miller, in Goldfarb et al., 1986), the Kenai Peninsula (Bradley et al., 1999), and the Matanuska Glacier area (Little and Naeser, 1989) (Fig. 13). Several of the hotter areas reached amphibolite facies, which is recognized in graywacke protoliths by the relatively low-pressure assemblage biotite > muscovite + andalusite ± cordierite ± garnet (Miller, in Goldfarb et al., 1986). Areas of amphibolite-facies metamorphism in the southern Kenai Peninsula (Seldo-

via quadrangle; Bradley et al., 1999) are concentrically zoned around ca. 56 Ma plutons and clearly are contact aureoles; metamorphic textures indicate that pluton emplacement was syntectonic (Fig. 10).

Ductile deformation that accompanied high-grade metamorphism has been best documented in the Chugach metamorphic complex, where Pavlis and Sisson (1995) recognized the following structural sequence. The first deformation consisted of imbrication and shortening of Valdez Group turbidites. When traced beyond the Chugach metamorphic complex, this deformation can be seen to have taken place at chlorite grade and to correspond to the main accretion-related deformation that is characteristic of Upper Cretaceous flysch units of the Chugach–Prince William terrane (e.g., Sample and Moore, 1987; Nokleberg et al., 1989). The two subsequent deformations (D2 and D3) were synchronous with the high-*T* metamorphism discussed above. D2 resulted in ductile, orogen-parallel extension, and in vertical shortening, which is indicated by recumbent folding of previously subvertical fabrics. D3 involved dextral transpression. Pavlis and Sisson (1995) identified four generations of Sanak-Baranof intrusives, the oldest of which predated D2 and accompanying metamorphism, and the youngest of which, north-striking dikes, are undeformed and were emplaced after D3.

EARLY TERTIARY EVENTS IN INTERIOR ALASKA

To this point we have focused on the accretionary prism. We now briefly discuss early Tertiary tectonism in areas located 150 to as much as 1000 km inboard of the paleotrench (Fig. 14). Episodes of basin subsidence, magmatism, and uplift took place at about the same time as near-trench magmatism, suggesting the possibility of genetic connections. Precise correlations between events in the accretionary prism and the interior, however, are hampered by uncertainties involving age control and the timing and magnitude of displacements on margin-parallel strike-slip faults (Miller et al., 2003).

Basin Subsidence

Several sedimentary basins in interior Alaska are approximately coeval with near-trench magmatism along the adjacent sector of the Sanak-Baranof belt. The Matanuska subbasin—one of two arms of Cook Inlet forearc basin at its northern end (location 15, Fig. 3)—underwent an episode of extension in early Tertiary time (Little and Naeser, 1989). The basin lay about 150 km landward of the paleotrench during the early Tertiary. Just prior to the time of interest, Upper Cretaceous shales and turbidites of the Matanuska Formation were being deposited in the forearc basin. These marine strata are disconformably overlain by nonmarine conglomerate, sandstone, shale, and coal of the Paleocene to Eocene Chickaloon Formation. Alluvial-fan conglomerates along the southern flank of the basin contain clasts of the McHugh Complex (Little, 1988); the Chugach–Prince William accretionary prism must therefore have risen above sea level by this time. Little and Naeser (1989) showed that north-dipping normal faults were active during deposition of the Chickaloon Formation along the southern basin margin. Three volcanic ash horizons interbedded with coal in the upper part of the Chickaloon Formation have yielded ages of 53.3 ± 1.5 to 55.8 ± 1.7 Ma (plagioclase K/Ar and zircon fission track, respectively; Triplehorn et al., 1984). The Talkeetna Mountains, which flank the Matanuska subbasin on the north, also rose during the early Tertiary. This is recorded by northerly derived boulder conglomerates of the Arkose Ridge Formation (Trop and Ridgway, 1999). The Arkose Ridge is assigned a late Paleocene through early Eocene age based on fossil plants (Silberman and Grantz, 1984) and on conventional K/Ar ages from intercalated basalt (50.0 ± 2.5, 51.8 ± 1.6, and 56.2 ± 1.7 Ma—all whole rock) and rhyolite (50.5 ± 1.5 whole rock, 45.5 ± 1.8 whole rock, and 51.4 ± 1 K-feldspar) (Winkler, 1992). A belt of Jurassic(?) mica schist (Winkler, 1992) just to the north has yielded $^{40}Ar/^{39}Ar$ white-mica ages of 59.7 ± 0.3 Ma (near-plateau) and 56.6 ± 0.2 Ma (plateau) (S. Harland and L. Snee, 2001, written commun.). Simultaneous extension and bimodal volcanism in the Matanuska subbasin and exhumation of metamorphic rocks in flanking highlands (location 22, Fig. 3) suggests that the southern Talkeetna Mountains may represent a core complex. Subject to the limitations of the geochronology, extension in the forearc basin would appear to have been coeval with near-trench magmatism along the adjacent part of the Sanak-Baranof belt (e.g., 54 Ma Crow Pass pluton) (Fig. 4).

Approximately 400 km inboard of the paleotrench, in the Alaska Range, the Cantwell Basin (Fig. 14) entered its second of two evolutionary stages at about the same time. During the first stage in Late Cretaceous time, the Cantwell Basin had been the site of fluvial deposition; it has been interpreted as a thrust-top basin formed in response to northward convergence between the Wrangellia composite terrane and previously accreted terranes to the north (Ridgway et al., 1997). The second stage, during the late Paleocene to earliest Eocene, was marked by mixed mafic and felsic volcanism and nonmarine sedimentation. The volcanic rocks range in age from 59 Ma at the base to 55 Ma at the top ($^{40}Ar/^{39}Ar$ biotite ages; Cole et al., 1999). This second phase of Cantwell Basin evolution broadly correlates with near-trench magmatism, and may be related to an episode of dextral motion along the Denali fault system (Figs. 1 and 14) (Miller et al., 2003).

Approximately 600 km inboard of the paleotrench, the Ruby-Rampart basin (Kirschner, 1994) (Fig. 14) is located along the Victoria Creek fault, a strand of the Kaltag strike-slip fault system. Its fill consists of nonmarine sandstone, conglomerate, coal, basalt, and rhyolite. Several of the volcanic rocks have yielded Paleocene $^{40}Ar/^{39}Ar$ ages: A rhyolite has been dated at 56 Ma (whole rock); a basalt at 60 Ma (whole rock); two mafic dikes at 58 and 59 Ma (whole rock); and two quartz-syenite dikes at 57.2 (biotite) and 57.8 Ma (whole rock) (P. Layer, quoted in Reifenstuhl et al., 1997). The basin is flanked

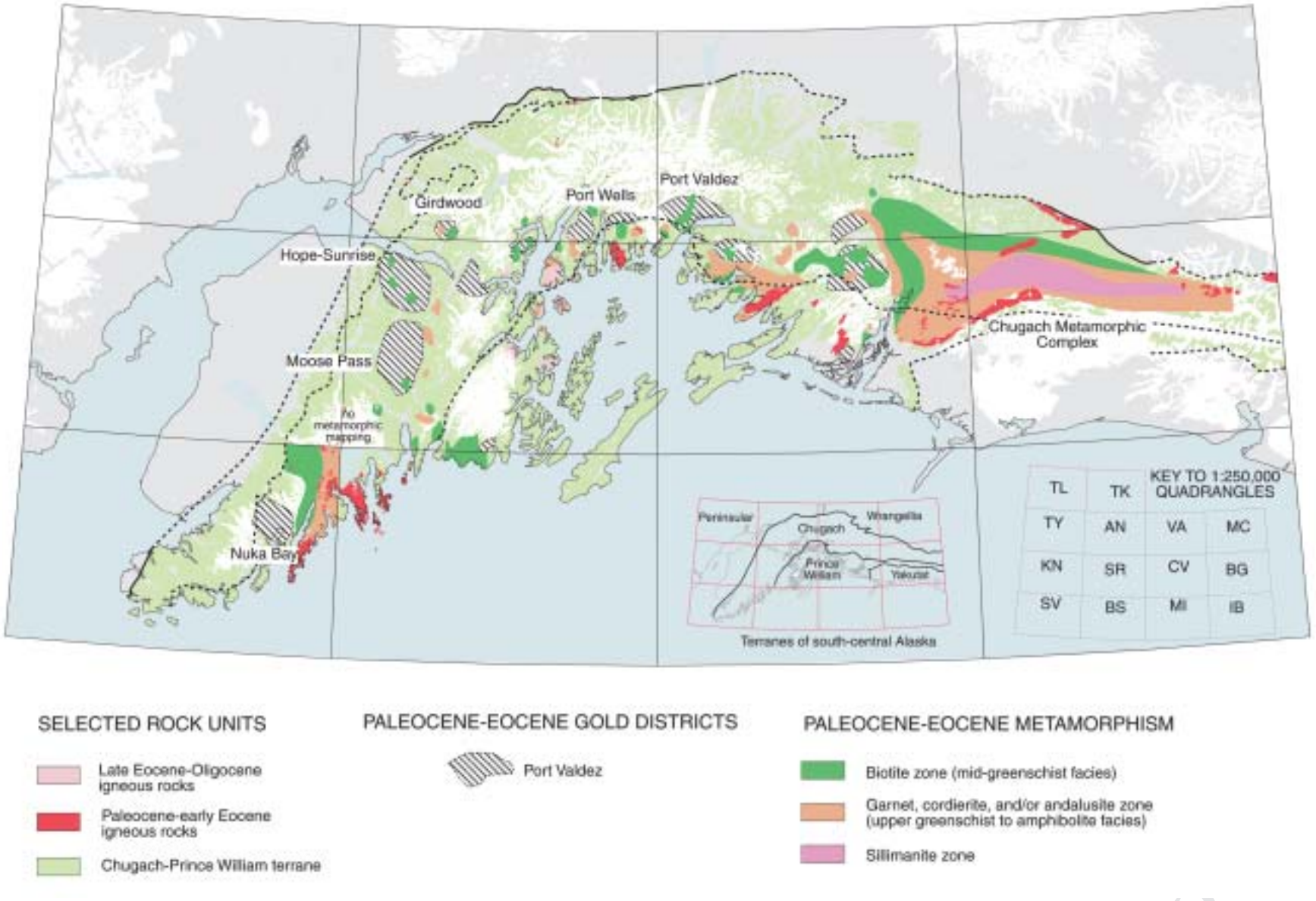

Figure 13. Map of the Chugach–Prince William terrane showing areas of anomalous, high-*T* metamorphism (from Sisson et al., 1989; Miller in Goldfarb et al., 1986; and Bradley et al., 1999), ca. 55 Ma gold districts (from Goldfarb et al., 1986), and near-trench plutonic rocks. The spotty map pattern of isograds results, in part, from the reconnaissance nature of metamorphic mapping.

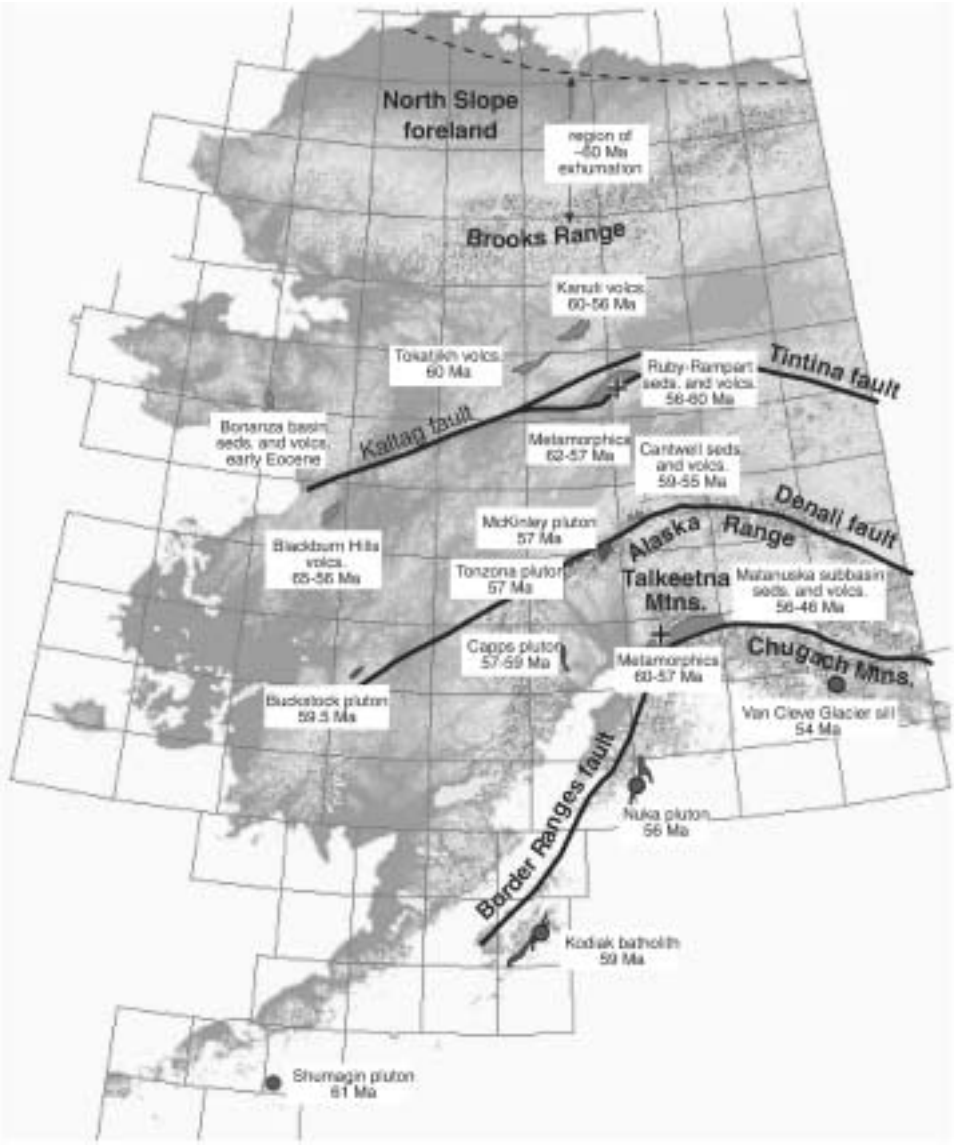

Figure 14. Map of Alaska showing selected Paleocene-Eocene plutons, volcanic centers, basins, metamorphic rocks, and other features. The four best-dated plutons of this portion of the Sanak-Baranof belt show the timing of near-trench magmatism. Note synchonism of various events in interior Alaska and near-trench magmatism. Detailed interpretation of interior events is hampered, however, by the still-controversial offsets across the margin-parallel strike-slip faults. Large (many hundreds of kilometers) dextral offsets since ca. 55 Ma would require comparing a particular location in the backstop with a no-longer adjacent part of the Sanak-Baranof belt.

to the southeast by a fault-bounded belt of anomalously young metamorphic rocks (mica schist, amphibolite, marble, and quartzite), which have yielded $^{40}Ar/^{39}Ar$ ages of 62 Ma (white mica) and 57 Ma (hornblende). Reifenstuhl et al. (1997) interpreted this unit as Ruby terrane or Yukon-Tanana terrane basement (Paleozoic protolith, metamorphosed in Jurassic to Early Cretaceous) that was rapidly exhumed during early Tertiary extension. Simultaneous basin subsidence, bimodal volcanism, and exhumation of metamorphic rocks within a strike-slip fault system suggests a transtensional core complex.

Magmatism

The interval from ca. 75 Ma to 58 Ma was characterized by widespread subduction-generated magmatism in the Alaska Range and backarc magmatism in the Kuskokwim region (Moll-Stalcup, 1994). In the Alaska Range (Fig. 1), the interval from 58 to 55 Ma was marked by emplacement of the McKinley series of plutons—peraluminous granites that Lanphere and Reed (1985) interpreted as products of partial melting of Mesozoic flysch in the unnamed collisional orogen north of the Wrangellia composite terrane. A magmatic lull then ensued, which was to last from ca. 55 to 40 Ma (Wallace and Engebretson, 1984). North of the Alaska Range, the 66–47 Ma Yukon-Kanuti magmatic belt includes several volcanic fields that overlap the age of near-trench magmatism along the adjacent Sanak-Baranof belt. The following description is from Moll-Stalcup (1994) and the rock units discussed are shown in Figure 14. The Kanuti field consists of dacite, andesite, and rhyodacite flows, domes, and tuffs erupted between 59.5 and 55.9 Ma. Similarly, the Tokatjikh field consists of andesite and dacite dated at 59.6 ± 0.6 Ma. The Blackburn Hills field consists

of andesite flows dated at 65 Ma near the base, which toward the top are interbedded with rhyolite domes and basalt flows, and intruded by 56 Ma granodiorite. The upper part of the Blackburn Hills succession shows a change from calc-alkalic ("arc-type") to mildly alkalic ("post-arc-type") compositions ca. 56 Ma (Moll-Stalcup, 1994).

Uplift of the Brooks Range and North Slope

Apatite fission track studies reveal that 1000 km inboard of the trench, the Brooks Range and the North Slope foreland basin (Fig. 1) were exhumed during Paleocene time (O'Sullivan et al., 1997). Rocks in the central Brooks Range cooled rapidly through 110–50 °C during discrete episodes at ca. 100 ± 5, ca. 60 ± 4, and ca. 24 ± 3 Ma. Foreland-basin strata just to the north record cooling pulses at ca. 60 ± 4, 46 ± 3, 35 ± 2, and ca. 24 ± 3 Ma. The 60 Ma event came after 40 million years of quiescence that had followed after collision-related Brookian shortening, and is notable because both the orogen and its proximal foreland were affected—a pairing that requires a mechanism other than thrust loading.

EARLY TERTIARY TECTONIC MODELS FOR ALASKA

We are now in a position to more thoroughly consider the various tectonic scenarios mentioned in the Introduction. Any viable model will need to account for the full range of coeval early Tertiary events in the accretionary prism: near-trench magmatism; low-pressure, high-temperature metamorphism; brittle and ductile deformation; ophiolite genesis; and trench sedimentation. Events in the Alaskan interior are less constraining for tectonic models because they can only be loosely tied to events along the coast; a successful tectonic model nonetheless should account for these events, at least qualitatively.

Eight possible explanations for near-trench magmatism—all involving subduction along the Gulf of Alaska margin—are explored below. The final three are variants of each other.

Arc magmatism. Kienle and Turner (1976) interpreted the near-trench plutons as the roots of an arc that had migrated to an extreme near-trench position. Even if the near-trench location might be explained in terms of very steep subduction, the arc model does not account for the diachronous age trend, nor for a coeval magmatic belt ~200–300 km farther inland along what had been the arc axis in latest Cretaceous time (Wallace and Engebretson, 1984). For a brief time, the seaward and landward belts coexisted, then magmatism tapered off in both.

Spontaneous melting of flysch. Hudson et al. (1979) regarded the Sanak-Baranof granitoids as anatectic melts of recently accreted trench sediments. At best, this is only a partial explanation, because the gabbroic plutons and basaltic dikes of the Sanak-Baranof belt—volumetrically minor though they are—require a mantle source. Moreover, spontaneous near-trench melting is not happening at any of the thickly sedimented Neogene accretionary prisms of the modern world (e.g., Makran, Cascadia, Barbados). The spontaneous anatectic melting model also fails to account for the fact that the latest Cretaceous flysch is the same age along the 2200 km length of the belt, yet there is a ten million–year difference between magmatism at the either end of the belt. Finally, this model provides no driving mechanism for deformation of the accretionary prism.

Trench-hotspot encounter. Another possible cause of near-trench magmatism is overriding a sea-floor hot spot. Two lines of evidence argue against this model. The first involves the age and location of magmatism. Overriding a hotspot would be expected to cause magmatism in only one place in an accretionary prism, not along its entire length. Only in the contrived case where the trend of the subduction zone was parallel to the relative motion of the overriding plate in a hot-spot reference frame would near-trench magmatism be diachronous along strike. Second, the distinctive alkalic signature of hotspot magmas are lacking.

Slab breakoff. This idea would entail the failure of what had been a single, subducting oceanic plate. The more deeply subducted part of the plate would have broken away and descended into the deep mantle, leaving, in its wake, a slab window. Slab breakoff has been suggested in a number of collisional orogens—the result of jamming a subduction zone with buoyant lithosphere—but to our knowledge has not been demonstrated for any oceanic subduction zones.

Flexural extension of a subducting plate. Tysdal et al. (1977) suggested that the Resurrection and Knight Island ophiolites formed by a variant of seafloor spreading when a single subducting plate was flexed upon entering a trench. Flexural extension, however, only effects the upper crust of a bending plate, so a clear mechanism for partial melting of the mantle would have been lacking.

Ridge subduction. Subduction of an active ridge-transform system, our preferred model, provides a single, unifying explanation for near-trench magmatism, low-pressure metamorphism, deformation, and hydrothermal activity, geology of the ophiolites, and the history of trench sedimentation and volcanism.

Subduction of very young seafloor. Melting of the accretionary prism might perhaps have been a consequence of subduction of very young ocean floor, but here the distinction blurs with the ridge subduction model, because very young ocean floor implies the nearby presence of even younger (zero-age) ocean floor at a spreading ridge.

Subduction of a "leaky transform." This mechanism, proposed by Tysdal et al. (1977) to explain the Resurrection and Knight Island ophiolites, also is merely a variant on the ridge subduction model because all spreading ridges have transform offsets and fracture-zone extensions.

RIDGE SUBDUCTION / SLAB WINDOW MODEL

On a global mosaic of two dozen large and small plates, divergent and convergent plate boundaries inevitably will intersect. The term "ridge subduction" describes the entry of a

oceanic spreading center into a subduction zone; it is not to be confused with "aseismic ridge subduction," which applies to such things as seamount chains that are embedded in a single subducting plate. A spreading center, as such, ceases to exist once it enters a subduction zone. In its place, an ever-widening "slab window" opens downdip of the trench (e.g., Thorkelson, 1996). This window is the interface between the base of the overriding plate and hot asthenosphere that wells up from beneath the two subducted, but still diverging plates. Several triple junction types can result from the intersection between broadly divergent and broadly convergent plate boundaries (Thorkelson, 1996). The simplest and most fundamental type, associated with subduction of ridge segments along a spreading system, is the trench-ridge-trench triple junction (e.g., Figs. 15A and 15C). The Chile triple junction, where South America is overriding the spreading center between the Nazca and Antarctic plates, is the best modern example of the trench-ridge-trench geometry (e.g., Cande and Leslie, 1986). Ridges are commonly offset by transforms, and when one of these enters a trench, the result is a trench-transform-trench triple junction (Fig. 15B). This still qualifies as "ridge subduction" in the loose sense that we favor. Two triple junctions along the western margin of North America represent special cases of "ridge subduction" in which one of the oceanic plates—in this case the Pacific—is moving parallel to the subduction zone, giving rise to trench-ridge-transform and trench-transform-transform triple junctions. The principles of ridge subduction have been examined by DeLong and Fox (1977), Dickinson and Snyder (1979), Thorkelson and Taylor (1989), Hole et al. (1991) and most thoroughly, by Thorkelson (1996).

Subduction of a ridge-transform system seems to account for the wide range of early Tertiary events in Alaska, particularly in the accretionary prism (Fig. 16). Ridge subduction elegantly accounts for the existence and diachronous age progression of near-trench magmatism (Bradley et al., 1993). Because triple junctions migrate, any effects of ridge subduction *should* be diachronous along the strike of a subduction zone, except in the two special cases where the ridge is either exactly parallel or exactly perpendicular to the subduction zone. A subducting ridge accounts for interbedded flysch and pillow lavas in the early Tertiary Resurrection ophiolite (Nelson et al., 1989; Bol et al., 1992; Kusky and Young, 1999), and for submarine volcanics interbedded with the Orca and Ghost Rocks flysch sequences (Moore et al., 1983). Such a ridge could have provided the heat source for the anomalous low-pressure, high-temperature metamorphism in the Chugach metamorphic complex (Sisson and Pavlis, 1993), and a way of generating and moving gold-bearing hydrothermal fluids in the accretionary prism (Haeussler et al., 1995). A ridge-trench encounter is likely to result in deformation, due to indentation of the accretionary prism, to changes in upper-plate rheology, and to changes in subduction direction. Extension and magmatism in the Alaskan interior are entirely consistent with subduction of a ridge and attendant opening of a slab window.

IMPLICATIONS OF THE SANAK-BARANOF TRIPLE JUNCTION FOR PLATE RECONSTRUCTIONS

Identity of Subducted Plates

Although tectonism along the Pacific rim of Alaska since the Cretaceous has undoubtedly been related to plate motions in the Pacific, the identity of the oceanic plates that have bordered Alaska is well established only since about the beginning of the Oligocene. Subduction of a vast tract of oceanic crust has obliterated the older marine magnetic anomalies that would provide the basis for unique plate reconstructions for the Late Cretaceous, Paleocene, and Eocene (Atwater, 1989). All Late Cretaceous to early Tertiary marine-based plate reconstructions show a Kula-Farallon spreading center that must have intersected the western margin North America somewhere—the question is where. Page and Engebretson (1984) handled this uncertainty by showing possible end-member locations for this trench-ridge-trench triple junction, a northern option in Washington (Fig. 17A), and a southern option in Mexico (the choice does not affect Alaska one way or the other, because both are so far south).

The near-trench plutons in Alaska provide onshore geologic evidence that a trench-ridge-trench triple junction existed along the continental margin—but in rocks now located some 3000 km along strike to the north of Page and Engebretson's (1984) northern option. Most workers have nonetheless interpreted the Sanak-Baranof near-trench magmatic belt as the consequence of subduction of the Kula-Farallon ridge (e.g., Marshak and Karig, 1977; Hill et al., 1981; Helwig and Emmett, 1981; Bradley et al., 1993; Haeussler et al., 1995; Sisson and Pavlis, 1993) (Fig. 17B). This is the most obvious choice of ridge as it is the only one that is required to have then existed in the northern Pacific but whose location is subject to conjecture. An alternative—permitted by the vanished magnetic anomaly record—is that yet another spreading ridge was responsible (Bradley et al., 1993; Miller et al., 2003; Haeussler et al., 2000, 2003); such a ridge would have separated the Kula plate from a hypothetical plate to the east (Fig. 17C). We suggest the name Resurrection plate for this hypothesized plate, for the Resurrection Ophiolite, which would be a remnant of it. In the "Resurrection plate" model, evidence for Paleocene-Eocene ridge subduction in Washington would be explained in terms of the Farallon-Resurrection ridge, whereas the Sanak-Baranof belt would be attributed to the Kula-Resurrection ridge. We now lean toward a configuration resembling that in Figure 17C, but acknowledge that a geometry like that in Figure 17B cannot be ruled out. In light of this ambiguity, it is probably best to refer to the site of inferred ridge subduction in Alaska as the "Sanak-Baranof triple junction." It bears repeating that some widely cited reconstructions show no ridge-trench encounter in Alaska between 61 and 50 Ma (e.g., Engebretson et al., 1984, 1985; Wallace and Engebretson, 1984; Plafker and Berg, 1994, their Fig. 5).

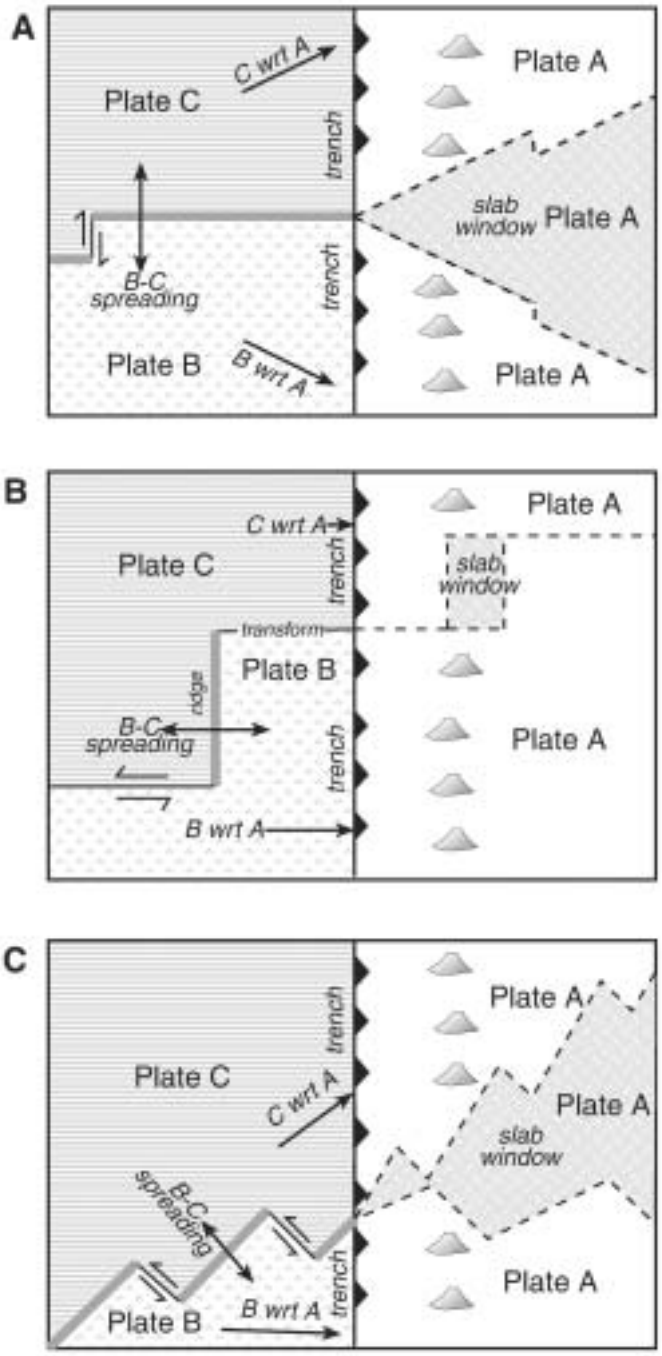

Figure 15. Schematic maps showing hypothetical interactions between ridge-transform systems and a convergent plate boundary. A: Ridge segments are perpendicular to the trench. A slab window opens between the subducted parts of the diverging plates. Were this gap at Earth's surface, new seafloor would have filled it; instead it is filled with hot asthenosphere that wells up to fill the vacancy. The trench-ridge-trench triple junction is stationary but will suddenly jump to a new position when the next transform reaches the trench. B: Ridge segments are parallel to the trench. A transform is being subducted; divergence across a previously subducted ridge segment has formed an isolated slab window at depth. The trench-transform-trench triple junction is stationary but will suddenly jump to a new position when the next ridge segment reaches the trench. C: Ridge segments are at an acute angle to the trench. The irregular shape of the slab window resulted from subduction of transform segments. The trench-ridge-trench triple junction will migrate southward until the next transform enters the trench, whereupon the triple junction will move back in the other direction. *C wrt A* and *B wrt A* are relative motions vectors. Adapted, in part, from Thorkelson (1996).

Palinspastic Complication #1: Oroclinal Bending

Formation of the southern Alaska orocline must also be accounted for in relating the Sanak-Baranof triple junction to plate reconstructions. Paleomagnetic data from a number of sites suggest that during the early Tertiary, southwestern Alaska rotated about 44° ± 11° counterclockwise with respect to cratonic North America (Coe et al., 1985, 1989). The time of oroclinal bending is bracketed between 66 and 44 Ma (Hillhouse and Coe, 1994)—but it is not known how much, if any, of the bending took place before, during, and after ridge subduction. Oroclinal rotation affected about half of the Chugach–Prince William terrane, along with its near-trench plutons that record the position of the Sanak-Baranof triple junction. Two quite different mechanisms for bending have been suggested. One possibility, implied by Coe et al. (1989), is that the hinge and eastern limb remained nearly fixed with respect to stable North America, while the western limb rotated southward. In this scenario, but depending also on the age of northward translation of the Chugach–Prince William terrane, the Sanak pluton could have moved as much as 1000 km *southward* during oroclinal rotation. An alternative possibility (Scholl et al., 1992) is that the orocline formed by indentation of an originally straighter margin, the hinge region corresponding to the indented area. In this case, the Sanak end of the belt would *not* have moved south with respect to North America. This choice between mechanisms is important to early Tertiary tectonic reconstructions because some plutons that track the Sanak-Baranof triple junction might or might not have moved considerable distances—before, during, or after ridge subduction. There are so many possible combinations that the chances of guessing correctly are poor.

Palinspastic Complication #2: Northward Terrane Transport

Paleomagnetic and geologic data each provide evidence, some of it conflicting, on the amount of northward movement of outboard terranes in Alaska. Some paleomagnetic studies have been interpreted to show very large (1000–4000 km) northward translations that were presumably taken up on margin-parallel strike-slip faults (e.g., Irving et al., 1996; Cowan et al., 1997). Most important to the present discussion is the amount of coastwise translation of the Chugach–Prince William

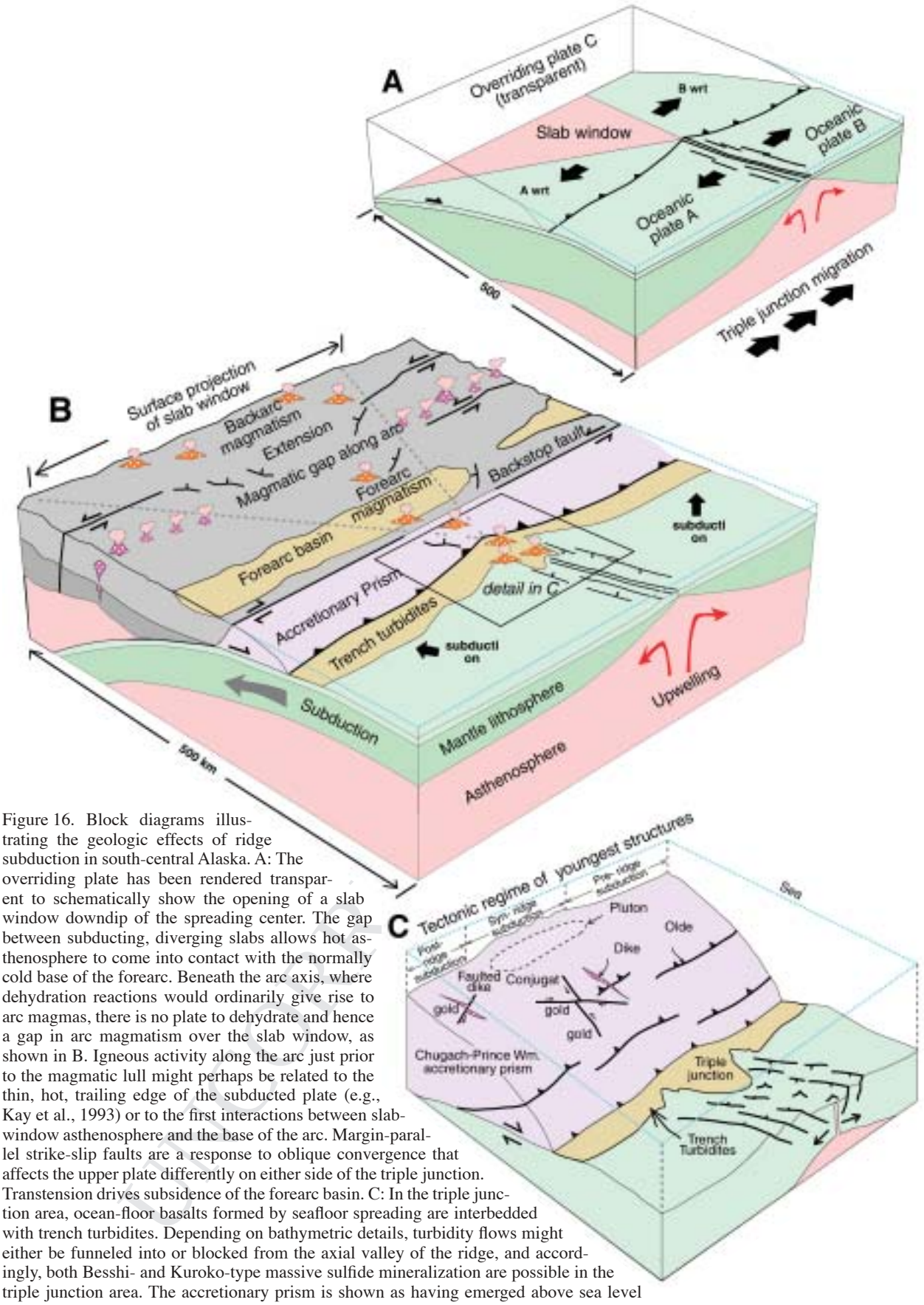

Figure 16. Block diagrams illustrating the geologic effects of ridge subduction in south-central Alaska. A: The overriding plate has been rendered transparent to schematically show the opening of a slab window downdip of the spreading center. The gap between subducting, diverging slabs allows hot asthenosphere to come into contact with the normally cold base of the forearc. Beneath the arc axis, where dehydration reactions would ordinarily give rise to arc magmas, there is no plate to dehydrate and hence a gap in arc magmatism over the slab window, as shown in B. Igneous activity along the arc just prior to the magmatic lull might perhaps be related to the thin, hot, trailing edge of the subducted plate (e.g., Kay et al., 1993) or to the first interactions between slab-window asthenosphere and the base of the arc. Margin-parallel strike-slip faults are a response to oblique convergence that affects the upper plate differently on either side of the triple junction. Transtension drives subsidence of the forearc basin. C: In the triple junction area, ocean-floor basalts formed by seafloor spreading are interbedded with trench turbidites. Depending on bathymetric details, turbidity flows might either be funneled into or blocked from the axial valley of the ridge, and accordingly, both Besshi- and Kuroko-type massive sulfide mineralization are possible in the triple junction area. The accretionary prism is shown as having emerged above sea level landward of the triple junction. The presence of near-trench, forearc volcanoes is inferred by analogy with the Woodlark triple junction; only near-trench plutons and dikes remain at the crustal levels now exposed in Alaska. Brittle faults, some of them mineralized by gold-quartz veins, facilitate orogen-normal shortening (i.e., the narrowing of the prism) and orogen-parallel extension.

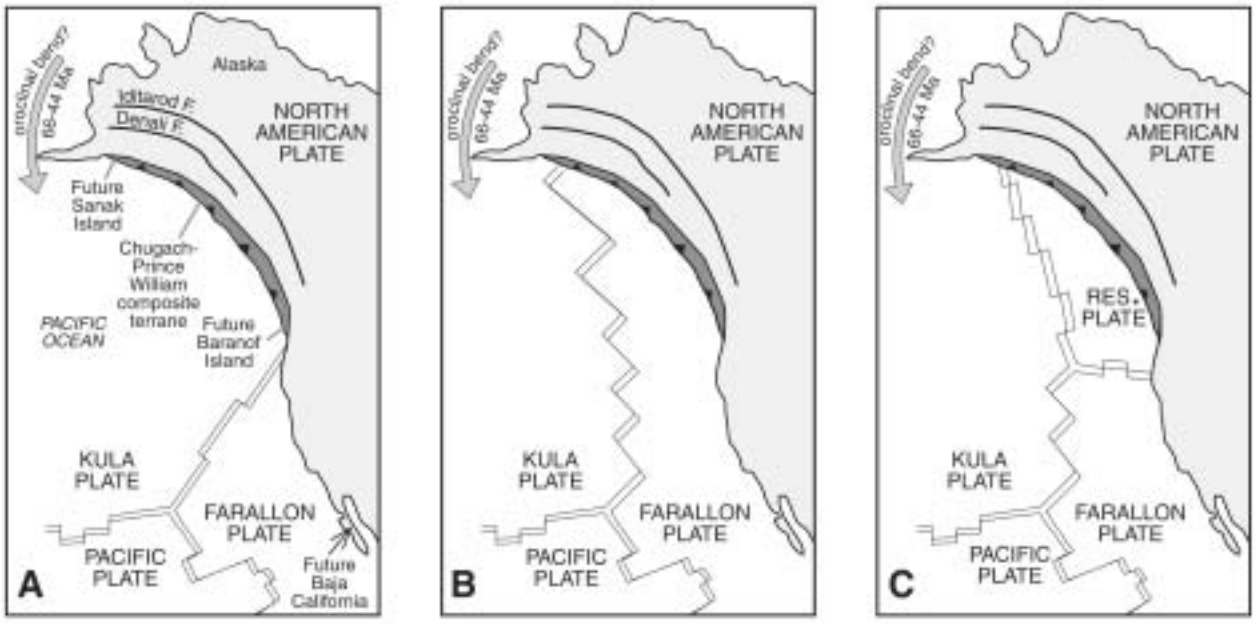

Figure 17. Alternative plate reconstructions. In each, the southern Alaska orocline has been somewhat straightened and the Chugach–Prince William terrane has been restored ~820 km southward along the margin. A: Kula-Farallon ridge intersects North America at the position of Engebretson et al.'s (1985) "northern option." B: Kula-Farallon ridge intersects the Chugach–Prince William terrane (modified by Bradley et al., 1993, from a diagram by Bol et al., 1992). C: Preferred model: a variant on B in which the ridge intersecting the Chugach–Prince William terrane separated the Kula plate from a previously unrecognized plate to the east, which we have named the Resurrection plate (Haeussler et al., 2000; Miller et al., 2003).

terrane (Fig. 1), and particularly its near-trench plutons, which record the position of the Sanak-Baranof trench-ridge-trench triple junction. For reconstructing the global plate mosaic, the key issue is restoration of the Chugach–Prince William terrane with respect to cratonic North America—the craton being the starting point of a multiplate reconstruction circuit. In order to link inboard and outboard events in Alaska, however, a more intricate puzzle must be solved, involving timing and amount of motion on all the significant margin-parallel faults. Two paleomagnetic results are particularly relevant to repositioning the Sanak-Baranof triple junction. Paleomagnetic data have been interpreted to indicate 13° ± 9° of northward displacement of the Chugach–Prince William terrane since 57 Ma (Bol et al., 1992). Allowing for the 325° strike of the margin, this equates to a coast-parallel translation of ~1745 ± 1205 km, or a range of about 540 to 2950 km. It bears noting, however, that Bol et al.'s (1992) paleomagnetic data are from the Resurrection Peninsula ophiolite (Fig. 1), which is interpreted to have been formed at a spreading ridge some distance offshore from earlier accreted parts of the Chugach–Prince William terrane. An unknown, but conceivably large, fraction of the northward travel of the Resurrection Peninsula thus took place before it was even part of the accretionary wedge (Kusky and Young, 1999). Paleomagnetic data from the more inland Wrangellia composite terrane in south-central Alaska show no latitudinal discrepancy with respect to North America as far back as 65–55 Ma (Hillhouse and Coe, 1994).

Geologic evidence from western Canada and eastern Alaska suggests approximately 450 km of dextral displacement across the Tintina fault (Dover, 1994) and approximately 370 km across the Denali fault east of the oroclinal hinge (Lowey, 1998) (Fig. 1). These distances are consistent with the paleomagnetic data from the Chugach–Prince William terrane, but at odds with the paleomagnetic data from the Wrangellia composite terrane, which also lies outboard of the Tintina and Denali faults. Total offset across the Border Ranges fault (i.e., the inboard boundary of the Chugach–Prince William terrane) is debatable, but available evidence allows only minor offset since the Sanak-Baranof belt formed. In southeastern Alaska, mapping by Johnson and Karl (1985) showed that a near-trench intrusion, the ca. 51 Ma Lake Elfendahl pluton (Table 1), crosscuts the fault, sealing this segment since early Eocene. Similarly, Little and Naeser (1989) identified a loose sedimentary linkage across the Border Ranges fault in south-central Alaska, which suggests at most only a few tens of kilometers of dextral offset between the two since the early Eocene. On the other hand, Roeske et al. (this volume, Chapter 6) have reported evidence for perhaps 700–1000 km dextral motion between Late Cretaceous and middle Eocene, and Smart et al. (1996) suggested as much as 600 km dextral offset based on the notion that 120 Ma plutonic rocks found on either side of the fault restore to a single cluster. Acknowledging that no interpretation can satisfy all the geologic and paleomagnetic data, in the following discussion, we use geologic offsets on all faults totaling 820 km.

Plate Geometry and Kinematics

Subject to straightening of the orocline and restoration of 820 km of dextral offset along the margin, Sanak Island would have lain in a position near the present Kenai Peninsula at 61 Ma, the onset of near-trench magmatism. If the Sanak-Baranof triple junction involved the Kula plate and the hypothesized Resurrection plate to the east (Fig. 17C), it would imply that the Resurrection plate would have been subducted before 61 Ma, the Kula plate from 61 to 43 Ma, and the Pacific plate since then. Alternatively, if the Sanak-Baranof triple junction involved the Kula and Farallon plates (Fig. 17B), the Farallon plate would have been subducted beneath Sanak Island until 61 Ma, the Kula plate subducted from 60 to 43 Ma, and the Pacific plate since then. As the ridge-transform system approached the subduction zone, minor plates would undoubtedly have formed; these would have been akin to today's Juan de Fuca and Gorda plates—small remnants of the once-vast Farallon plate.

No direct evidence exists for the configuration of ridges and transforms along the subducted ridge but transform segments almost certainly would have existed. Paleomagnetic declinations from sheeted dikes of the Resurrection Peninsula suggest that the ridge trended 026° ± 12° (Bol et al., 1992); transforms would thus have trended 116° ± 12°. The Sanak-Baranof belt includes "hotter" sectors within which intrusive rocks and/or high-temperature metamorphic rocks are abundant, separated by relatively "colder" areas. This might reflect, at least in part, the subduction of ridge segments versus transform segments. Sisson and Pavlis (1993), Pavlis and Sisson (1995), and Poole (1996) have suggested that some of the complicated history of the Chugach metamorphic complex might have been due to backtracking of the triple junction along the continental margin in connection with ridge-transform complexities.

The nature of tectonism along the margin just before and just after near-trench magmatism suggests that the Sanak-Baranof triple junction was the trench-ridge-trench type, as opposed to, for example, a trench-ridge-transform type. This is best documented on Kodiak Island and adjacent islands. In the latest Cretaceous and earliest Paleocene, deposition of thick turbidite sequences (Kodiak and Ghost Rocks Formations) was followed within a few million years by penetrative deformation, including melange formation, and then by near-trench plutonism. Immediately outboard of the belts containing near-trench intrusions are accreted Eocene turbidites (Sitkalidak Formation) that are themselves deformed and unconformably overlain by undeformed Oligocene strata (Moore and Allwardt, 1980). The style and sequence of deformations of the Kodiak, Ghost Rocks, and Sitkalidak Formations has been widely interpreted in terms of subduction-accretion along a convergent margin (Byrne, 1984; Sample and Moore, 1987).

As a subducting ridge passes a point along a convergent margin, the direction of subduction abruptly changes. Depending on the angle between the ridge and margin, the sense of subduction obliquity might also change. Such is the case at the present-day Chile Triple Junction, which marks a divide between dextral and sinistral margin-parallel strike-slip faults in the forearc (Kay et al., 1993). In Alaska, however, dextral strike slip would appear to have taken place before, during, and after the inferred ridge subduction event. Roeske et al. (this volume, Chapter 6) have described evidence for dextral motion on the Hanagita strand of the Border Ranges fault system between ca. 85 and ca. 51 Ma, which spans the time when the triple junction is inferred to have migrated past this part of the margin. Passage of the Sanak-Baranof triple junction coincided with episodes of margin-parallel strike slip elsewhere, as well. In the Matanuska subbasin (location 15, Fig. 3), Little (1988) has shown that dextral strike slip on the Border Ranges fault system was coeval with emplacement of dacite dikes that he correlated with similar dikes of the Sanak-Baranof belt. In the Chugach metamorphic complex (Fig. 2), D3 deformation took place relatively late in the near-trench high-*T* sequence, and involved dextral transpression (Pavlis and Sisson, 1995). As discussed earlier, subsidence and volcanism in the Cantwell and Ruby-Rampart basins are consistent with episodes of strike slip on the Denali and Kaltag faults, respectively (Fig. 1). Finally, in southeastern Alaska, gold mineralization on margin-parallel dextral faults was coeval with near-trench magmatism, and all strike-slip faults that postdate gold-quartz veins are dextral. To the extent that margin-parallel strike slip faithfully records subduction obliquity, subduction of both the leading and trailing oceanic plates would appear to have had a dextral-oblique component.

Some recent attempts have been made to fine-tune the plate reconstructions of Engebretson et al. (1984, 1985) in light of information from the Sanak-Baranof belt (e.g., Sisson and Pavlis, 1993; Pavlis and Sisson, 1995; Kusky and Young, 1999). The Engebretson et al. (1985) reconstructions were a major landmark but they are now in need of revision on several counts, irrespective of any new onshore geologic constraints: (1) mounting evidence has called into question the fixed hotspot assumption on which these reconstructions were based (e.g., Molnar and Stock, 1987; Tarduno and Cottrell, 1997); (2) new magnetic anomaly data and picks are available for virtually the entire world ocean, which will support more accurate North America–Africa–Antarctica–Pacific–Kula–Farallon plate circuits; and (3) significant revisions have been made to the magnetic polarity time scale (e.g., Gradstein et al., 1994; Berggren et al., 1995)—the basis for correlation between seafloor spreading history and onshore geology. Until a new generation of oceanic-plate reconstructions is available, improvements suggested by the Sanak-Baranof belt and triple junction are probably best left as hypothetical scenarios (Fig. 17).

IMPLICATIONS FOR RIDGE-SUBDUCTION PROCESSES

Ridge Subduction and Forearc Tectonics

Submarine accretionary prisms and subaerial contractional orogenic belts owe their critical taper to a balance between the strength of the wedge, basal friction, and basal and surface slopes (Davis et al., 1983; Platt, 1986). As a subducting ridge migrates

along a convergent margin, several mechanical effects might be expected in an accretionary prism. One effect is simply topographic: At 2.7 km below sea level, a spreading ridge is a high-standing, buoyant object rising far above normal ocean floor. The trench would be expected to shallow, then deepen, as a subducting ridge passes a particular location (DeLong and Fox, 1977). This effect can be seen in the Chile Trench, which systematically shallows toward the Chile triple junction (e.g., Thornburg and Kulm, 1987, their Fig. 2). Judging from the Chilean example, the bathymetric anomaly associated with the subducting ridge in Alaska could have been perhaps 3 km high and several thousand kilometers long. Geologic confirmation of this long-wavelength effect has not been specifically sought in Alaska, but anecdotal observations are at least consistent with what might be expected. Rise of the accretionary prism above sea level during late Paleocene or Eocene is recorded by detritus shed landward into the forearc basin (Little and Naeser, 1989). The paleocurrent patterns of turbidites deposited along or near the continental margin show a profound change at about the time of near-trench magmatism, which could have been due to bathymetric changes associated with the passage of the triple junction.

On a shorter wavelength, the subducting ridge crest itself is likely to induce shortening and uplift in the immediate vicinity of the triple junction. At the Chile triple junction, the ridge indents the inner trench wall (Forsythe and Prior, 1992), and a similar effect can be seen elsewhere in the world where aseismic ridges are presently being subducted (e.g., Cocos Ridge at the Middle American Trench; Corrigan et al., 1990). The structural evidence summarized above shows that margin-perpendicular shortening did take place in the accretionary prism at the time of ridge subduction in Alaska.

Another likely effect of ridge subduction involves a weakening of the accretionary prism as a result of heating, both advectively by rising magmas and conductively from hot asthenosphere of the slab window. The fact that the Chugach–Prince William accretionary prism was heated is self-evident from the extent of near-trench plutons (Fig. 2) and of areas of mid-greenschist and higher metamorphism (Fig. 13). In the Chugach metamorphic complex, D2 recumbent folds that Pavlis and Sisson (1995) attributed to vertical shortening might be attributed to a loss of strength of the prism. There is no evidence that the weakened prism extended in a seaward direction, but it did extend parallel to the margin in areas of both ductile and brittle deformation (Fig. 16). Eventually, as the triple junction moved on, it would have left in its wake an accretionary prism that cooled with time. The final outcome of ridge subduction in Alaska was an accretionary prism that was riddled with isotropic plutons armored by hornfels rims, undoubtedly stronger—and hence capable of sustaining a steeper critical taper—than before.

Magmatism Related to Ridge Subduction

Five igneous provinces in Alaska can be temporally linked to ridge subduction (Fig. 16B). The following list starts at the seaward end of a north-south transect in the vicinity of the oroclinal axis: (1) pillow basalts and andesites that are interbedded with trench deposits; (2) the near-trench plutons and dikes that are the main basis for the ridge-subduction model; (3) volcanics in the forearc basin; (4) the youngest plutons along the arc axis in the Alaska Range that predate a magmatic lull of about 15 million years; and (5) widespread volcanics in a continental backarc region. Each of these has potential analogues in the modern world.

The Knight Island and Resurrection Peninsula ophiolites are presumed to be analogous to ocean floor that is presently being produced at spreading centers that are about to be subducted, such as the Chile Rise and the Gorda Ridge. Sheeted dike complexes attest to an extensional tectonic setting. Interbedded turbidites within the pillow sequence suggest proximity to a trench. Trace-element data can be explained by sediment contamination of N-MORB-like magmas to yield arc-like trace element signatures (Crowe et al., 1992; Nelson and Nelson, 1993; Lytwyn et al., 1997). Off-axis igneous activity in the trench is perhaps represented by basaltic and andesitic flows that are interbedded with flysch sequences and are not associated with sheeted dike complexes. Such anomalous volcanism *on the downgoing plate* is the hallmark feature of ridge subduction east of New Guinea, where the Woodlark spreading center has encountered the Solomon Trench (Taylor and Exon, 1987).

The near-trench intrusive rocks provide the strongest evidence for ridge subduction. Trace-element and isotopic data are best interpreted in terms of melting of flysch at depth in the accretionary prism, the heat having been supplied by upwelling asthenosphere in the slab window. The forearc volcanoes shown in Figure 15 would be the extrusive equivalents of intrusive rocks seen today at the present level of exposure. Modern analogues are known from the Woodlark triple junction, where active volcanoes dot the trench and forearc (Taylor and Exon, 1987), and the Chile triple junction, where a near-trench granodiorite pluton has been dated at 3.6 Ma (Forsythe and Nelson, 1985; Forsythe et al., 1986). Paleocene to Eocene volcanic horizons in the Matanuska subbasin (location 15, Fig. 3) may represent the landward continuation of the Sanak-Baranof igneous province.

The age of arc magmatism in Alaska also can be explained in terms of ridge subduction. Igneous activity along the 74 to 55 Ma Alaska Range magmatic belt was followed by a magmatic lull from 55 to 40 Ma (Wallace and Engebretson, 1984), after which magmatism resumed. This sequence might be interpreted in terms of arc magmatism related to subduction of the leading plate (prior to ridge subduction) followed by passage of a slab window beneath the arc. By analogy, a volcanic gap in the Andean arc landward of the Chile triple junction corresponds closely to the predicted position of the slab window (Kay et al., 1993; Cande and Leslie, 1986). Plutons in the Alaska Range that just preceded the lull (e.g., McKinley Series of granitic rocks of Lanphere and Reed, 1985) would thus correlate with passage of the thin, hot, trailing edge of the subducted slab

beneath the arc. These plutons would be analogous to the most southerly volcano in the Southern Volcanic Belt in Chile (Kay et al., 1993), which is expected to be the next volcano to go extinct as the slab window migrates into a position beneath it. An alternative view is that the entire 80–45 Ma history of arc magmatism in Alaska was due to subduction of a single plate, the Kula (Bergman and Hudson, 1987); in our view, this does not account for near-trench magmatism.

Early Tertiary volcanic rocks north of the Alaska Range (e.g., Kanuti, Tokatjikh, and Blackburn Hills fields) correlate in part with magmatism in the adjacent sector of the Sanak-Baranof belt. Kay et al. (1993) and d'Orazio et al. (2000, 2001) have described Neogene continental backarc volcanics in Patagonia above the modern slab window associated with the Chile triple junction. The Patagonian volcanics, which occur as far as ~650 km from the trench, are potential analogs for the Alaskan volcanics.

Far-Field Uplift

Brief mention has been made of a Paleocene episode of exhumation in the Brooks Range and its proximal foreland, which permissibly overlaps the age of Sanak-Baranof magmatism in south-central Alaska. The question is whether or not a slab window could conceivably have affected an area located as far as 1000 km from the paleotrench. Fission track studies from Patagonia, landward of the Chile triple junction, show that Neogene ridge subduction has not caused denudation of the upper plate (Thomson et al., 2001). On the other hand, far-field uplift is predicted by geodynamic models of sublithospheric flow that inevitably takes place in the wedge of asthenosphere above a subducted slab and below an overriding plate (Mitrovica et al., 1989). Modeling revealed that protracted subduction of ocean floor in the Pacific would have caused long-wavelength (>1000 km), high-amplitude (1000 m) depression of both the Canadian Rockies and the associated foreland. Conversely, upon cessation of subduction (e.g., as a result of collision, or opening of a slab window), both orogen and foreland rebounded (Mitrovica et al., 1989).

CLOSING COMMENTS

Ridge subduction is not uncommon. On the present plate mosaic, there are six locations—each with its own geometry—where a ridge-transform system intersects a convergent margin. Moreover, because triple junctions migrate, a single ridge-transform system can eventually work its way along many hundreds to thousands of kilometers of convergent margin—the "moving blowtorch" effect. Ridge subduction was probably even more common in the deep past. For example, when the number of plates was about twice that at present near the end of the Archean (Abbott and Menke, 1990), ridge subduction would have been twice as common. Nonetheless, surprisingly few hypothesized ancient examples have yet been recognized, presumably for want of clear-cut criteria. Alaska is among the most prominent of the Tertiary examples and warrants continued research in the effort to recognize the geologic effects of ridge subduction.

ACKNOWLEDGMENTS

Much of the research reported here was conducted under the Alaska Mineral Resource Assessment Program of the U.S. Geological Survey. Haeussler was supported by a U.S. Geological Survey post-doctoral fellowship from 1992 to 1994. Kusky drew support from NSF Grant 9304647 for studies of near-trench plutonism. Collaborations with Randy Parrish, Larry Snee, Paul Layer, Dan Lux, Matt Heizler, and Bill Clendenen yielded many of the dates on which our interpretations now rest. Figure 3 was derived from digital geology provided in part by Nora Shew and Ric Wilson. Aaron Otteman assisted with geochronological compilations. Mark Brandon, Steve Bergman, Cynthia Dusel-Bacon, Don Richter, and Jinny Sisson provided insightful reviews. We thank editors Jinny Sisson, Sarah Roeske, and Terry Pavlis, for putting together this volume.

REFERENCES CITED

Atwater, T., 1989, Plate tectonic history of the northeast Pacific and western North America, *in* Winterer, E.L., et al., eds., The geology of North America: The eastern Pacific Ocean and Hawaii: Boulder, Colorado, Geological Society of America, Geology of North America, v. N, p. 21–72.

Abbott, D., and Menke, W., 1990, Length of the global plate boundary at 2.4 Ga: Geology, v. 18, p. 58–61.

Barker, F., Farmer, G.L., Ayuso, R.A., Plafker, G., and Lull, J.S., 1992, The 50 Ma granodiorite of the eastern Gulf of Alaska: Melting in an accretionary prism in the forearc: Journal of Geophysical Research, v. 97, p. 6757–6778.

Beikman, H., 1980, Geologic map of Alaska: U.S. Geological Survey, scale 1: 2,500,000.

Berggren, W.A., Kent, D.V., Swisher, C.C., III, and Aubry, M., 1995, A revised Cenozoic geochronology and chronostratigraphy: SEPM (Society for Sedimentary Geology) Special Publication No. 54, p. 144–139.

Bergman, S.C., and Hudson, T.L., 1987, Magmatic rock evidence for a Paleocene change in the tectonic setting of Alaska: Geological Society of America Abstracts with Programs, v. 19, no. 7, p. 586–587.

Bol, A.J., Coe, R.S., Gromme, C.S., and Hillhouse, J.W., 1992, Paleomagnetism of the Resurrection Peninsula, Alaska: Implications for the tectonics of southern Alaska and the Kula-Farallon Ridge: Journal of Geophysical Research, v. 97, p. 17,213–17,232.

Bradley, D.C., and Kusky, T.M., 1990, Kinematics of late faults along Turnagain Arm, Mesozoic accretionary complex, south-central Alaska: U.S. Geological Survey Bulletin 1946, p. 3–10.

Bradley, D.C., and Kusky, T.M., 1992, Deformation history of the McHugh Complex, Seldovia quadrangle, south-central Alaska: U.S. Geological Survey Bulletin 1999, p. 17–32.

Bradley, D.C., Haeussler, P., and Kusky, T.M., 1993, Timing of Early Tertiary ridge subduction in southern Alaska: U.S. Geological Survey Bulletin 2068, p. 163–177.

Bradley, D.C., Kusky, T., Haeussler, P., Karl, S., and Donley, D.T., 1999, Geologic map of the Seldovia quadrangle, Alaska: U.S. Geological Survey Open-File Report 99-18, scale 1:250,000.

Bradley, D.C., Parrish, R., Clendenen, W., Lux, D., Layer, P., Heizler, M., and Donley, D.T., 2000, New geochronological evidence for the timing of early Tertiary ridge subduction in southern Alaska: U.S. Geological Survey Professional Paper 1615, p. 5–21.

Byrne, T., 1984, Early deformation in mélange terranes of the Ghost Rocks Formation, Kodiak Islands, Alaska, *in* Raymond, L.A., ed., Melanges: Their

nature, origin, and significance: Boulder, Colorado, Geological Society of America Special Paper 198, p. 21–51.

Cande, S.C., and Leslie, R.B., 1986, Late Cenozoic tectonics of the southern Chile Trench: Journal of Geophysical Research, v. 91, p. 471–496.

Coe, R.S., Globerman, B.R., Plumley, P.R., and Thrupp, G.A., 1985, Paleomagnetic results from tectonic implications, *in* Howell, D.G., ed., Tectonostratigraphic terranes of the circum-Pacific region: Houston, Texas, Circum-Pacific Council for Energy and Mineral Resources, Earth Science Series, v. 1, p. 85–108.

Coe, R.S., Globerman, B.R., Plumley, P.R., and Thrupp, G.A., 1989, Rotation of central and southern Alaska in the Early Tertiary: Oroclinal bending by megakinking?, *in* Kissel, C., and Laj, C., eds., Paleomagnetic rotations and continental deformation: Boston, Kluwer Academic Publishers, NATO-ASI series, p. 327–339.

Cole, R.B., Ridgway, K.D., Layer, P.W., and Drake, J., 1999, Kinematics of basin development during the transition from terrane accretion to strike-slip tectonics, Late Cretaceous–early Tertiary Cantwell Formation, south-central Alaska: Tectonics, v. 18, p. 1224–1244.

Connelly, W., 1978, Uyak Complex, Kodiak Islands, Alaska: A Cretaceous subduction complex: Geological Society of America Bulletin, v. 89, p. 755–769.

Corrigan, J., Mann, P., and Ingle, J.C., Jr., 1990, Forearc response to subduction of the Cocos Ridge, Panama–Costa Rica: Geological Society of America Bulletin, v. 102, p. 628–652.

Cowan, D.S., Brandon, M.T., and Garver, J.I., 1977, Geologic tests of hypotheses for large coastwise displacements—A critique illustrated by the Baja British Columbia hypothesis: American Journal of Science, v. 297, p. 117–173.

Crowe, D.E., Nelson, S.W., Brown, P.E., Shanks, W.C., III, and Valley, J.W., 1992, Geology and geochemistry of volcanogenic massive sulfide deposits and related igneous rocks, Prince William Sound, southern Alaska: Economic Geology, v. 87, p. 1722–1746.

Davis, D., Suppe, J., and Dahlen, F.A., 1983, Mechanics of fold-and-thrust belts and accretionary wedges: Journal of Geophysical Research, v. 88, p. 1153–1172.

Decker, J.E., 1980, Geology of a Cretaceous subduction complex, western Chichagof Island, southeastern Alaska [Ph.D. thesis]: Stanford, California, Stanford University, 135 p.

DeLong, S.E., and Fox, P.J., 1977, Geologic consequences of ridge subduction: American Geophysical Union, Maurice Ewing Series, v. 1, p. 221–228.

Dickinson, W.R., and Snyder, W.S., 1979, Geometry of subducted slabs related to the San Andreas transform: Journal of Geology, v. 87, p. 609–627.

d'Orazio, M., Agostini, S., Mazzarini, F., Innocenti, F., Manetti, P., Haller, M.J., and Lahsen, A., 2000, The Pali Aike Volcanic Field, Patagonia: Slab-window magmatism near the tip of South America: Tectonophysics, v. 321, p. 407–427.

d'Orazio, M., Agostini, S., Innocenti, F., Haller, M.J., Manetti, P., and Mazzarini, F., 2001, Slab window–related magmatism from southernmost South America: The Late Miocene mafic volcanics from the Estancia Glencross area (~52° S, Argentina-Chile): Lithos, v. 57, p. 67–89.

Dover, J.H., 1994, Geology of part of east-central Alaska, *in* Plafker, G., and Berg, H.C., eds., The geology of Alaska: Boulder, Colorado, Geological Society of America, Geology of North America, v. G-1, p. 153–204.

Dumoulin, J.A., 1987, Sandstone composition of the Valdez and Orca Groups, Prince William Sound, Alaska: U.S. Geological Survey Bulletin 1774, 37 p.

Dumoulin, J.A., 1988, Sandstone petrographic evidence and the Chugach–Prince William terrane boundary in southern Alaska: Geology, v. 16, p. 456–460.

Dusel-Bacon, C., Csejtey, B., Jr., Foster, H.L., Doyle, E.O., Nokleberg, W.J., and Plafker, G., 1993, Distribution, facies, ages, and proposed tectonic associations of regionally metamorphosed rocks in east- and south-central Alaska: U.S. Geological Survey Professional Paper 1497-C, p. C1–C72.

Engebretson, D.C., Cox, A., and Gordon, R.G., 1984, Relative motions between oceanic plates of the Pacific Basin: Journal of Geophysical Research, v. 89, p. 10,291–10,310.

Engebretson, D.C., Cox, A., and Gordon, R.G., 1985, Relative motions between oceanic and continental plates in the Pacific Basin: Boulder, Colorado, Geological Society of America Special Paper 206, 59 p.

Ferry, J.M., 1981, Petrology of graphitic sulfide-rich schists from south-central Maine: An example of desulfidation during prograde regional metamorphism: American Mineralogist, v. 66, p. 908–930.

Forsythe, R.D., and Nelson, E.P., 1985, Geological manifestations of ridge collision: Evidence from the Golfo de Penas-Taitao basin, southern Chile: Tectonics, v. 4, p. 477–495.

Forsythe, R.D., Nelson, E.P., Carr, M.J., Kaeding, M.E., Herve, M., Mpodozis, C., Soffia, J.M., and Harambour, S., 1986, Pliocene near-trench magmatism in southern Chile: A possible manifestation of ridge collision: Geology, v. 14, p. 23–27.

Forsythe, R., and Prior, D., 1992, Cenozoic continental geology of South America and its relations to the evolution of the Chile Triple Junction: Proceedings of the Ocean Drilling Program, Initial reports, Volume 141: College Station, Texas, Ocean Drilling Program, p. 23–31.

Goldfarb, R.J., Leach, D.L., Miller, M.L., and Pickthorn, W.J., 1986, Geology, metamorphic setting, and genetic constraints of epigenetic lode-gold mineralization within the Cretaceous Valdez Group, south-central Alaska: Geological Association of Canada Special Paper 32, p. 87–105.

Goldfarb, R.J., Miller, L.D., Leach, D.L., and Snee, L.W., 1997, Gold deposits in metamorphic rocks in Alaska: Economic Geology Monograph 9, p. 151–190.

Gradstein, F.M., Agterberg, F.P., Ogg, J.G., Hardenbol, J., van Veen, P., Thierry, J., and Huang, Zehui, 1994, A Mesozoic time scale: Journal of Geophysical Research, v. 99, p. 24,051–24,074.

Haeussler, P.J., and Bradley, D.C., 1993, Map and compilation of structural data from lode-gold mineral occurrences in the Chugach–Prince William terrane of southern Alaska: U.S. Geological Survey Open-File Report 93-325, 53 p., 1 plate.

Haeussler, P.J., Bradley, D.C., Goldfarb, R., and Snee, L., 1995, Link between ridge subduction and gold mineralization in southern Alaska: Geology, v. 23, p. 995–998.

Haeussler, P.J., Bradley, D.C., Miller, M.L., and Wells, R., 2000, Life and death of the Resurrection plate: Evidence for an additional plate in the NE Pacific in Paleocene-Eocene time: Geological Society of America Abstracts with Programs, v. 32, no. 7, p. A-382.

Haeussler, P.J., Bradley, D.C., Wells, R., and Miller, M.L., 2003, Life and death of the Resurrection plate: Evidence for an additional plate in the northeastern Pacific in Paleocene-Eocene time: Geological Society of America Bulletin, v. 115, p. 867–880.

Haeussler, P.J., Bradley, D.C., and Goldfarb, R.J., 2003, Brittle deformation along the Gulf of Alaska margin in response to Paleocene-Eocene triple junction migration, *in* Sisson, V.B., Roeske, S.M., and Pavlis, T.L., eds, Geology of a transpressional orogen developed during ridge-trench interaction along the North Pacific margin: Boulder, Colorado, Geological Society of America Special Paper 371, p. X–XX (this volume).

Harris, N.R., Sisson, V.B., Wright, J.E., and Pavlis, T.E., 1996, Evidence for Eocene mafic underplating during forearc intrusive activity, eastern Chugach Mountains, Alaska: Geology, v. 24, p. 263–266.

Helwig, J., and Emmet, P., 1981, Structure of the Early Tertiary Orca Group in Prince William Sound and some implications for the plate tectonic history of southern Alaska: Journal of the Alaska Geological Society, v. 1, p. 12–35.

Hill, M., Morris, J., and Whelan, J., 1981, Hybrid granodiorites intruding the accretionary prism, Kodiak, Shumagin, and Sanak Islands, southwest Alaska: Journal of Geophysical Research, v. 86, p. 10,569–10,590.

Hillhouse, J.W., and Coe, R.S., 1994, Paleomagnetic data from Alaska, *in* Plafker, G., and Berg, H.C., eds., The geology of Alaska: Boulder, Colorado, Geological Society of America, Geology of North America, v. G-1, p. 797–812.

Himmelberg, G.R., Loney, R.A., and Nabelek, P.I., 1987, Petrogenesis of gabbronorite at Yakobi and northwest Chichagof Islands, Alaska: Geological Society of America Bulletin, v. 98, p. 265–279.

Hole, M.J., Rogers, G., Saunders, A.D., and Storey, M., 1991, Relation between alkalic volcanism and slab window formation: Geology, v. 19, p. 657–660.

Hudson, T., 1983, Calc-alkaline plutonism along the Pacific rim of southern Alaska, *in* Roddick, J.A., ed., Circum-Pacific plutonic terranes: Boulder, Colorado, Geological Society of America Memoir 159, p. 159–169.

Hudson, T., and Plafker, G., 1982, Paleogene metamorphism in an accretionary flysch terrane, eastern Gulf of Alaska: Geological Society of America Bulletin, v. 93, p. 1280–1290.

Hudson, T., Plafker, G., and Peterman, Z.E., 1979, Paleogene anatexis along the Gulf of Alaska margin: Geology, v. 7, p. 573–577.

Irving, E., Wynne, P.J., Thorkelson, D.J., and Schiarizza, P., 1996, Large (1000 to 4000 km) northward movements of tectonic domains in the Northern Cordillera, 83 to 45 Ma: Journal of Geophysical Research, v. 101, p. 17,901–17,916.

Johnson, B.R., and Karl, S.M., 1985, Geologic map of western Chichagof and Yakobi Islands, southeastern Alaska: U.S. Geological Survey Map MI-1506, scale 1:125,000, 15 p.

Karl, S.M., Zumsteg, C., Haeussler, P.J., and Himmelberg, G.R., 1999, Slab window metamorphism of the Chugach accretionary complex, Baranof

Island, southeastern Alaska: Eos (Transactions, American Geophysical Union), v. 80, p. F1025.

Kay, S.M., Ramos, V.A., and Márquez, 1993, Evidence in Cerro Pampa volcanic rocks for slab-melting prior to ridge-collision in southern South America: Journal of Geology, v. 101, p. 703–714.

Kienle, J., and Turner, D.L., 1976, The Shumagin-Kodiak batholith—A Paleocene magmatic arc?, *in* Short notes on Alaskan geology, 1976: Alaska Division of Geological and Geophysical Surveys Geologic Report 51, p. 9–11.

Kirschner, C.E., 1994, Interior basins of Alaska, *in* Plafker, G., and Berg, H.C., eds., The geology of Alaska: Boulder, Colorado, Geological Society of America, Geology of North America, v. G-1, p. 469–493.

Kusky, T.M., and Young, C.M., 1999, Emplacement of the Resurrection Peninsula ophiolite in the southern Alaska forearc during a ridge-trench encounter: Journal of Geophysical Research, v. 104, p. 29,025–29,054.

Kusky, T.M., Bradley, D.C., and Haeussler, P., 1997a, Progressive deformation of the Chugach accretionary complex, Alaska, during a Paleogene ridge-trench encounter: Journal of Structural Geology, v. 19, p. 139–157.

Kusky, T.M., Bradley, D.C., Haeussler, P., and Karl, S.J., 1997b, Controls on accretion of flysch and melange belts at accretionary margins: Evidence from the Chugach Bay thrust and Iceworm melange, Chugach accretionary wedge, Alaska: Tectonics, v. 16, p. 855–878.

Kusky, T.M., Bradley, D., Donley, D.T., Rowley, D., and Haeussler, P., 2003, Controls on intrusion of near-trench magmas of the Sanak-Baranof Belt, Alaska, during Paleogene ridge subduction, and consequences for forearc evolution, *in* Sisson, V.B., Roeske, S.M., and Pavlis, T.L., eds, Geology of a transpressional orogen developed during ridge-trench interaction along the North Pacific margin: Boulder, Colorado, Geological Society of America Special Paper 371, p. X–XX (this volume).

Lanphere, M.A., and Reed, B.L., 1985, The McKinley sequence of granitic rocks: A key element in the accretionary history of southern Alaska: Journal of Geophysical Research, v. 90, p. 11,413–11,430.

LeBas, M.J., LeMaitre, R.W., Streckeisen, A., and Zanettin, B., 1986, A chemical classification of volcanic rocks based on the total alkali silica diagram: Journal of Petrology, v. 27, p. 745–750.

Little, T.A., 1988, Tertiary tectonics of the Border Ranges fault system, north-central Chugach Mountains, Alaska: Sedimentation, deformation, and uplift along the inboard edge of a subduction complex [Ph.D. thesis]: Stanford, California, Stanford University, 343 p.

Little, T.A., and Naeser, C.W., 1989, Tertiary tectonics of the Border Ranges fault system, Chugach Mountains, Alaska: Deformation and uplift in a forearc setting: Journal of Geophysical Research, v. 94, p. 4333–4359.

Loney, R.A., and Brew, D.A., 1987, Regional thermal metamorphism and deformation of the Sitka Graywacke, southern Baranof Island, southeastern Alaska: U.S. Geological Survey Bulletin 1779, 17 p.

Loney, R.A., and Himmelberg, G.R., 1983, Structure and petrology of the La Perouse gabbro intrusion, Fairweather Range, southeastern, Alaska: Journal of Petrology, v. 24, p. 377–423.

Lowey, G.W., 1998, A new estimate of the amount of displacement on the Denali fault system based on the occurrence of carbonate megaboulders in the Dezadeash Formation (Jura-Cretaceous), Yukon, and the Nutzotin Mountains sequence (Jura-Cretaceous), Alaska: Bulletin of Canadian Petroleum Geology, v. 46, p. 379–386.

Lull, J.S., and Plafker, G., 1990, Geochemistry and paleotectonic implications of metabasaltic rocks in the Valdez Group, southern Alaska: U.S. Geological Survey Bulletin 1946, p. 29–38.

Lytwyn, J., Casey, J., Gilbert, S., and Kusky, T., 1997, Arc-like mid-ocean ridge basalt formed seaward of a trench-forearc system just prior to ridge subduction: An example from subaccreted ophiolites in southern Alaska: Journal of Geophysical Research, v. 102, p. 10,225–10,243.

Lytwyn, J., Casey, J., Gilbert, S., and Kusky, T., 2000, Geochemistry of near-trench intrusive rocks associated with ridge subduction, Seldovia quadrangle, southern Alaska: Journal of Geophysical Research, v. 105, p. 27,957–27,978.

Marshak, R.S., and Karig, D.E., 1977, Triple junctions as a cause for anomalously near-trench igneous activity between the trench and volcanic arc: Geology, v. 5, p. 233–236.

Miller, M.L., 1984, Geology of the Resurrection Peninsula, *in* Winkler, G.L., et al., eds., Guide to the bedrock geology of a traverse of the Chugach Mountains from Anchorage to Cape Resurrection: Alaska Geological Society Guidebook, p. 25–34.

Miller, M.L., Bradley, D.C., and Bundtzen, T.K., and McClelland, W., 2002, Late Cretaceous through Cenozoic strike-slip tectonics of southwestern Alaska: Journal of Geology, v. 110, p. 247–270.

Mitrovica, J.X., Beaumont, C., and Jarvis, G.T., 1989, Tilting of continental interiors by the dynamical effects of subduction: Tectonics, v. 8, p. 1079–1094.

Moll-Stalcup, E.J., 1994, Latest Cretaceous and Cenozoic magmatism in mainland Alaska, *in* Plafker, G., and Berg, H.C., eds., The geology of Alaska: Boulder, Colorado, Geological Society of America, Geology of North America, v. G-1, p. 589–619.

Molnar, P., and Stock, J.M., 1987, Relative motions of hotspots in the Pacific, Atlantic, and Indian Oceans since Late Cretaceous time: Nature, v. 327, p. 587–591.

Moore, J.C., 1973, Cretaceous continental margin sedimentation, southwestern Alaska: Geological Society of America Bulletin, v. 84, p. 595–614.

Moore, J.C., and Allwardt, A., 1980, Progressive deformation of a Tertiary trench slope, Kodiak islands, Alaska: Journal of Geophysical Research, v. 85, p. 4741–4756.

Moore, J.C., Byrne, T., Plumley, P.W., Reid, M., Gibbons, H., and Coe, R.S., 1983, Paleogene evolution of the Kodiak Islands, Alaska: Consequences of ridge-trench interaction in a more southerly latitude: Tectonics, v. 2, p. 265–293.

Nelson, S.W., and Nelson, M.S., 1993, Geochemistry of ophiolitic rocks from Knight Island, Prince William Sound, Alaska: U.S. Geological Survey Bulletin 2068, p. 130–142.

Nelson, S.W., Dumoulin, J.A., and Miller, M.L., 1985, Geologic map of the Chugach National Forest, Alaska: U.S. Geological Survey Miscellaneous Field Studies Map MF-1645-B, 14 p., 1 sheet, scale 1:250,000.

Nelson, S.W., Miller, M.L., and Dumoulin, J.A., 1989, Resurrection Peninsula ophiolite, *in* Nelson, S.W., and Hamilton, T.W., eds., Guide to the geology of Resurrection Bay, eastern Kenai Fiords area, Alaska: Anchorage, Geological Society of Alaska, p. 10–20.

Nilsen, T.H., and Moore, G.W., 1979, Reconnaissance study of Upper Cretaceous to Miocene stratigraphic units and sedimentary facies, Kodiak and adjacent islands, Alaska: U.S. Geological Survey Professional Paper 1093, 34 p.

Nilsen, T.H., and Zuffa, G.G., 1982, The Chugach terrane, a Cretaceous trench-fill deposit, southern Alaska: Geological Society [London] Special Publication No. 10, p. 213–227.

Nokleberg, W.J., Plafker, G., Lull, J.S., Wallace, W.K., and Winkler, G.R., 1989, Structural analysis of the southern Peninsular, southern Wrangellia, and northern Chugach terranes along the Trans-Alaska Crustal Transect, northern Chugach Mountains, Alaska: Journal of Geophysical Research, v. 94, p. 4297–4320.

Nokleberg, W.J., Plafker, G., and Wilson, F.H., 1994, Geology of south-central Alaska, *in* Plafker, G., and Berg, H.C., eds., The geology of Alaska: Boulder, Colorado, Geological Society of America, Geology of North America, v. G-1, p. 311–366.

Onstott, T.C., Sisson, V.B., and Turner, D.L., 1989, Initial argon in amphiboles from the Chugach Mountains, southern Alaska: Journal of Geophysical Research, v. 94, p. 4361–4372.

O'Sullivan, P.B., Murphy, J.M., and Blythe, A.E., 1997, Late Mesozoic and Cenozoic thermotectonic evolution of the central Brooks Range and adjacent North Slope foreland basin, Alaska: Including fission-track results from the Trans-Alaska Crustal Transect (TACT): Journal of Geophysical Research, v. 102, p. 20,821–20,845.

Page, B.M., and Engebretson, D.C., 1984, Correlation between the geologic record and computed plate motions for central California: Tectonics, v. 3, p. 133–155.

Pavlis, T.L., and Sisson, V.B., 1995, Structural history of the Chugach metamorphic complex in the Tana River region, eastern Alaska: A record of Eocene ridge subduction: Geological Society of America Bulletin, v. 107, p. 1333–1355.

Plafker, G., and Berg, H.C., 1994, Overview of the geology and tectonic evolution of Alaska, *in* Plafker, G., and Berg, H.C., eds., The geology of Alaska: Boulder, Colorado, Geological Society of America, Geology of North America, v. G-1, p. 989–1021.

Plafker, G., Moore, J.C., and Winkler, G.R., 1994, Geology of the southern Alaska margin, *in* Plafker, G., and Berg, H., eds., The geology of Alaska: Boulder, Colorado, Geological Society of America, Geology of North America, v. G-1, p. 389–449.

Platt, J.P., 1986, Dynamics of orogenic wedges and the uplift of high-pressure metamorphic rocks: Geological Society of America Bulletin, v. 97, p. 1037–1053.

Poole, A.R., 1996, Age and geochemical constraints on ridge subduction for igenous rocks of the eastern Chugach Mountains, Alaska [master's thesis]: Houston, Texas, Rice University, 83 p.

Reifenstuhl, R.R., 1986, Geology of the Goddard Hot Springs area, Baranof Island, southeastern Alaska: Alaska Division of Geological and Geophysical Surveys, Public-Data File 86-2, 82 p., 1 plate, scale 1:40,000.

Reifenstuhl, R.R., Dover, J.H., Newberry, R.J., Clautice, K.H., Liss, S.A., Blodgett, R.B., Bundtzen, T.K., and Weber, F.R., 1997, Interpretive bedrock geologic map of the Tanana B1 quadrangle, central Alaska: Alaska Division of Geological and Geophysical Surveys, Report of Investigations 97-15B, 15 p., scale 1:63,360.

Richter, D.H., 1965, Geology and mineral deposits of central Knight Island, Prince William Sound, Alaska: Alaska Division of Mines and Minerals, Geologic Report 16, 37 p.

Ridgway, K.D., Trop, J.M., and Sweet, A.R., 1997, Thrust-top basin formation along a suture zone, Cantwell basin, Alaska Range: Implications for development of the Denali fault system: Geological Society of America Bulletin, v. 109, p. 505–523.

Roeske, S.M., Snee, L.W., Pavlis, T.L., 2003, Dextral-slip reactivation of an arc-forearc boundary during Late Cretaceous–Early Eocene oblique convergence in the northern Cordillera, *in* Sisson, V.B., Roeske, S.M., and Pavlis, T.L., eds, Geology of a transpressional orogen developed during ridge-trench interaction along the North Pacific margin: Boulder, Colorado, Geological Society of America Special Paper 371, p. X–XX (this volume).

Sample, J.C., and Moore, J.C., 1987, Structural style and kinematics of an underplated slate belt, Kodiak and adjacent islands, Alaska: Geological Society of America Bulletin, v. 99, p. 7–20.

Scholl, D.W., Stevenson, A.J., Mueller, S., Geist, E., Engebretson, D.C., and Vallier, T.L., 1992, Exploring the notion that southeast-Asian-type escape tectonics and trench clogging are involved in regional-scale deformation of Alaska and the formation of the Aleutian-Bering Sea region, *in* Southeast Asia structure, tectonics and magmatism: Geodynamics Research Institute Symposium, College Station, Texas, Program and Abstracts, Texas A&M University, p. 57–61.

Silberman, M.L., and Grantz, A., 1984, Paleogene volcanic rocks of the Matanuska Valley and the displacement history of the Castle Mountain fault: U.S. Geological Survey Circular 868, p. 82–86.

Sisson, V.B., and Pavlis, T.L., 1993, Geologic consequences of plate reorganization: An example from the Eocene southern Alaska forearc: Geology, v. 21, p. 913–916.

Sisson, V.B., Hollister, L.S., and Onstott, T.C., 1989, Petrologic and age constraints on the origin of a low-pressure/high-temperature metamorphic complex, southern Alaska: Journal of Geophysical research, v. 94, p. 4392–4410.

Smart, K.J., Pavlis, T.L., Sisson, V.B., Roeske, S.M., and Snee, L.W., 1996, The Border Ranges fault system in Glacier Bay National Park, Alaska: Evidence for major early Cenozoic dextral strike-slip motion: Canadian Journal of Earth Sciences, v. 33, p. 1268–1282.

Sisson, V.B., Poole, A.R., Harris, N.R., Cooper Burner, H., Pavlis, T.L., Copeland, P., Donelick, R.A., and McLelland, W.C., 2003, Geochemical and geochronologic constraints for genesis of a tonalite-trondhjemite suite and associated mafic intrusive rocks in the eastern Chugach Mountains, Alaska: A record of ridge-transform subduction, *in* Sisson, V.B., Roeske, S.M., and Pavlis, T.L., eds, Geology of a transpressional orogen developed during ridge-trench interaction along the North Pacific margin: Boulder, Colorado, Geological Society of America Special Paper 371, p. X–XX (this volume).

Streckeisen, A.L., 1973, Plutonic rocks; classification and nomenclature recommended by the IUGS subcommision on the systematics of igneous rocks: Geotimes, v. 18, p. 26–30.

Sun, S.-S., 1980, Lead isotopic study of young volcanic rocks from mid-ocean ridges, ocean islands, and volcanic arcs: Royal Society of London Philosophical Transactions, v. 297, p. 409–445.

Sun, S.-S., and McDonough, W.F., 1989, Chemical and isotopic systematics of oceanic basalts: Implications for mantle compositions and processes, *in* Saunders, A.D., and Norry, M.J., eds., Magmatism in the ocean basins: Geological Society [London] Special Publication No. 42, p. 313–345.

Tarduno, J.A., and Cottrell, R.D., 1997, Paleomagnetic evidence for motion of the Hawaiian hotspot during formation of the Emperor seamounts: Earth and Planetary Science Letters, v. 153, p. 171–180.

Taylor, B., and Exon, N.F., 1987, An investigation of ridge subduction in the Woodlark-Solomons region: Introduction and overview, *in* Taylor, B., and Exon, N., eds., Marine geology, geophysics, and geochemistry of the Woodlark Basin-Solomon Islands: Houston, Texas, Circum-Pacific Council for Energy and Mineral Resources, Earth Science Series, v. 7, p. 1–24.

Taylor, C.D., Goldfarb, R.J., Snee, L.W., Gent, C.A., Karl, S.M., and Haeussler, P.J., 1994, New age data for gold deposits and granites, Chichagof Mining District, SE Alaska: Evidence for a common origin: Geological Society of America Abstracts with Programs, v. 26, no. 7, p. A-140.

Thomson, S.N., Hervé, F., and Stöckert, B., 2001, Mesozoic-Cenozoic denudation history of the Patagonian Andes (southern Chile) and its correlation to different tectonic processes: Tectonics, v. 20, p. 693–711.

Thorkelson, D.J., 1996, Subduction of diverging plates and principles of slab window formation: Tectonophysics, v. 255, p. 47–63.

Thorkelson, D.J., and Taylor, R.P., 1989, Cordilleran slab windows: Geology, v. 17, p. 833–836.

Thornburg, T.M., and Kulm, L.D., 1987, Sedimentation in the Chile Trench: Depositional morphologies, lithofacies, and stratigraphy: Geological Society of America Bulletin, v. 98, p. 33–52.

Triplehorn, D.M., Turner, D.L., and Naeser, C.W., 1984, Radiometric age of the Chickaloon Formation of south-central Alaska: Location of the Paleocene-Eocene boundary: Geological Society of America Bulletin, v. 95, p. 740–742.

Trop, J.M., and Ridgway, K.D., 1999, Sedimentology and provenance of the Paleocene-Eocene Arkose Ridge Formation, Cook Inlet–Matanuska Valley forearc basin, southern Alaska: Alaska Division of Geological and Geophysical Surveys, Professional Report 119, p. 129–144.

Trop, J.M., Ridgway, K.D., and Spell, T.L., 2003, Sedimentary record of transpressional tectonics and ridge subduction in the Tertiary Matanuska Valley–Talkeetna Mountains forearc basin, southern Alaska, *in* Sisson, V.B., Roeske, S.M., and Pavlis, T.L., eds, Geology of a transpressional orogen developed during ridge-trench interaction along the North Pacific margin: Boulder, Colorado, Geological Society of America Special Paper 371, p. X-XX (this volume).

Tysdal, R.G., and Case, J.E., 1979, Geologic map of the Seward and Blying Sound quadrangles, Alaska: U.S. Geological Survey Miscellaneous Investigations Series I-1150, 12 p., 1 sheet, scale 1:250,000.

Tysdal, R.G., Case, J.E., Winkler, G.R., and Clark, S.H.B., 1977, Sheeted dikes, gabbro, and pillow basalt in flysch of coastal southern Alaska: Geology, v. 5, p. 377–383.

Vrolijk, P., 1987, Tectonically driven fluid flow in the Kodiak accretionary complex, Alaska: Geology, v. 15, p. 466–469.

Wallace, W.K., and Engebretson, D.C., 1984, Relationships between plate motions and Late Cretaceous to Paleogene magmatism in southwestern Alaska: Tectonics, v. 3, p. 295–315.

Weinberger, J., and Sisson, V.B., 2003, Pressure and temperature conditions of brittle/ductile vein emplacement in the greenschist facies, Chugach metamorphic complex, Alaska: Evidence from fluid inclusions, *in* Sisson, V.B., Roeske, S.M., and Pavlis, T.L., eds, Geology of a transpressional orogen developed during ridge-trench interaction along the North Pacific margin: Boulder, Colorado, Geological Society of America Special Paper 371, p. X-XX (this volume).

Winkler, G.R., 1976, Deep-sea fan deposition of the lower Tertariy Orca Group, eastern Prince William Sound, Alaska, *in* Miller, T., ed., Recent and ancient sedimentary environments in Alaska: Alaska Geological Society Symposium Proceedings, p. R1–R20.

Winkler, G.R., 1992, Geologic map and summary geochronology of the Anchorage 1° × 3° quadrangle, southern Alaska: U.S. Geological Survey Map I-2283, scale 1:250,000.

Worrall, D.M., 1991, Tectonic history of the Bering Sea and the evolution of Tertiary strike-slip basins of the Bering shelf: Boulder, Colorado, Geological Society of America Special Paper 257, 120 p.

Zuffa, G.G., Nilsen, T.H., and Winkler, G.R., 1980, Rock-fragment petrography of the Upper Cretaceous Chugach terrane, southern Alaska: U.S. Geological Survey Open-File Report 80-713, 28 p.

Manuscript Accepted by the Society February 5, 2003

Printed in the USA